Main group metal lone-pair...π(arene) interactions: A new bonding mode for supramolecular associations†

Ignez Caracelli,[a] Julio Zukerman-Schpector,*[,b] Ionel Haiduc[c] and Edward R.T. Tiekink*[,d]

[a] BioMat, Departamento de Física, Universidade Federal de São Carlos, C.P. 676, São Carlos, São Paulo 13565-905, Brazil

[b] Laboratório de Cristalografia, Estereodinâmica e Modelagem Molecular, Departamento de Química, Universidade Federal de São Carlos, C.P. 676, São Carlos, SP 13565-905, Brazil. E-mail: julio@power.ufscar.br; Fax: +55 16 33518350; Tel: +55 16 33518208

[c] Facultatea de Chimie, Universitatea Babes-Bolyai, RO-400028 Cluj-Napoca, Romania

[d] Research Centre for Crystalline Materials, Faculty of Science and Technology, Sunway University, 47500 Bandar Sunway, Selangor Darul Ehsan, Malaysia. E-mail: edwardt@sunway.edu.my; Fax: +60 3 7491 8633; Tel: +60 3 7491 7173

Abstract

Crystal structures of the heavier main group elements in low oxidation states have been evaluated for the presence of supramolecular element(lp)···π(arene) interactions that are structure-directing. It is revealed that when present, these interactions lead to zero-dimensional, binuclear aggregates but higher-nuclearity species are sometimes observed, with one-dimensional supramolecular chains of varying topology being prominent. By contrast,

two-dimensional aggregation based on element(lp)···π(arene) interactions are rare. In summary, interactions of main group metal lone-pairs with aromatic rings are revealed as synthons capable of assembling molecules into supramolecular aggregates.

† Electronic supplementary information (ESI) available: For ESI (illustrations of supramolecular aggregation based on main group element(lone-pair)···π(arene) interactions for **1**–**157**), see DOI:

Introduction

It was in the realm of macromolecular crystallography that the concept of element(lone-pair)···π-system interactions most likely arose; hereafter lone-pair = lp. Thus, it was Egli and Gessner in their rationalisation of the structure of the left-handed Z-DNA duplex who concluded that cytidine-O(lp)···π(pyrimidinyl) interactions were crucial for the stabilisation of the observed conformation.[1] Subsequently, other light-atom structures were suggested to contain similar interactions in both protein[2] and molecular structural chemistry;[3] further discussion of the biological inspiration behind element(lp)···π-system interactions is given below. In terms of supramolecular chemistry, it is likely that the first mention of heavy element(lp)···π(arene) interactions was in a review of the structural chemistry of tellurium compounds.[4] Subsequently, a number of systematic bibliographic reviews have appeared over the last decade describing supramolecular architectures sustained by element(lp)···π-system interactions, including those having element = oxygen,[5] tin,[6] lead,[7] thallium,[8] arsenic,[9] antimony,[10] bismuth,[10] selenium[11] and tellurium.[11b,12] [1] The purpose of the present survey is to provide an update on the structures of the elements from tin to tellurium containing element(lp)···π(arene) interactions, since the appearance of their original literature survey, and to describe the supramolecular aggregates they stabilise. This is especially salient as it is still comparatively rare for mention of these contacts, let alone the aggregation patterns resulting from them, to be mentioned in the primary publication.

At first glance it might appear odd that element(lp)···π(arene) interaction might be considered as stabilising/attractive when both components might be considered electron-rich. While transition metal···π(arene) interactions are readily explained in terms of attraction between a metal and an π-electron cloud,[13] the same does not pertain for post-transition

[1] An overview of these reviews is to appear in a Chapter in "Aromatic Interactions: Frontiers in Knowledge and Application" Edited by Darren W. Johnson and Fraser Hof

elements which being in low oxidation states often possess stereochemically active lone-pair(s) of electrons. Under these circumstances, it is not surprising that such interactions have attracted the interest of theoreticians.[14] The rationale for the formation of element(lp)···π(arene) interactions is very similar to that proposed for halogen bond which, also at first glance, appears contrary to expectation.[15] Described simply, in either context, the distribution of electron density is asymmetric, there being a build-up of electron density about the middle bounds of the electron distribution leaving a region depleted of electron density at the end which may be variously termed an electropositive region, σ-hole or polar cap. In halogen bonding this would be located at the end of the vector of the, say, carbon–halogen bond. In the case of a lone-pair, the polar cap would be found at the tip of the lone-pair. It is the electrophilic polar cap that interacts with the electron density of the π-ring to form a stabilising interaction.

In keeping with the notion that identification of supramolecular synthons is a key element of crystal engineering,[16] in the following, after a brief outline of the protocols employed to ascertain the presence of element(lp)···π(arene) interactions in the crystal structures of the heavier main group elements, a systematic survey of structures having these interactions and the self-assembly based on these will be presented.

Methodology

The search protocols utilised for the current survey were adapted from those employed in earlier systematic surveys of element(lp)···π(arene) interactions.[5-12] The Cambridge Structural Database (CSD: version 5.37 + 2 updates)[17] was searched using CONQUEST (version 1.18).[18] The structural protocols are outlined in Fig. 1a, there being two key geometric restraints. The first relates to the distance, *d*, between the metal centre and the ring

centroid, Cg. Following recent literature precedents,[5-12] this was set at 4.0 Å to capture all reasonable contacts. Earlier work indicates that if an element(lp)···π(arene) interaction is to form, it will usually form at distances within the sum of the van der Waals radii of the element in question and that estimated for an arene ring, *i.e.* 1.9 Å.[19] The angle, θ, is the angle between the normal to the plane through the arene ring (V_1) and the vector passing through Cg to the element in question (V_2), and provides a sense of the relative location of the element above the plane. In the present survey, θ, was restricted to be ≤ 20º. This restriction ensures that only delocalised[20] element(lp)···π(arene) interactions were retrieved from the CSD, meaning approximately equal lp···C separations, Fig. 1b. This is in contrast to localised interactions, where the lone-pair is directed towards a single atom of the ring, and semi-localised interactions where the lone-pair is directed to one of the bonds of the ring.[20] Non-geometric restrictions were also applied. Thus, only neutral structures were considered and structures with R > 0.07, with unresolvable disorder, determined from powder data and those that are polymeric being omitted. Further, structures featuring element(lp)···π(arene) interactions but, where the arene ring was a solvent were also omitted.

Having a database of possible candidates for each structure, data were manually scrutinised to ensure that the element(lp)···π(arene) interaction in question was structure-directing, meaning that the interaction was operating in isolation of other intermolecular interactions, *e.g.* hydrogen bonding and secondary interactions. As an illustration of this, the analysis of the supramolecular association in the structure of {Pb[S_2P(O-iPr)(OC_6H_4OEt-4)]$_2$}[21] is given here. Referring to Fig. 2, the centrosymmetric aggregate is sustained by a pair of Pb(lp)···π(arene) interactions with *d* = 3.32 Å and θ = 9.2º, *i.e.* falling within the cited search criteria. However, this structure has been omitted from the survey as the Pb(lp)···π(arene) interactions are complemented by secondary Pb···S interactions and therefore cannot be considered as structure-directing, operating in isolation of other

supramolecular synthons. After manual sorting, there were a total of 157 new structures containing structure-directing elements(lp)···π(arene) interactions that have appeared since the original bibliographic review of each element; a small number of structures that were overlooked in the original surveys are also included here. The supramolecular aggregations patterns resulting from element(lp)···π(arene) interactions in **1-157** are discussed in the next section. Diagrams showing supramolecular aggregation are original and were drawn with DIAMOND.[22] Chemical diagrams were drawn with ChemDraw® with only species directly participating in element(lp)···π(arene) interactions illustrated. Geometric data are collated in Tables 1-5. The structure analysis program PLATON[23] was also routinely employed in the present survey.

Results

Preamble

The following is a succinct overview of supramolecular aggregation patterns sustained by M(lp)···π(arene) interactions which are structure-determining in that they are operating in isolation of other supramolecular synthons such as hydrogen bonding and secondary interactions. The supramolecular aggregates described herein were not covered in earlier reviews of similar interactions published over the last decade for tin,[6] lead,[7] thallium,[8] arsenic,[9] antimony,[10] bismuth,[10] selenium[11] and tellurium.[11b,12] compounds. The aggregates for each of the elements are arranged in terms of dimension, mono-, bi, tri-nuclear molecules, *etc*., number of unique M(lp)···π(arene) interactions and in the case of selenium and tellurium, oxidation state. Within each category, aggregates are ordered in terms of the value of *d* and then differentiated by θ in cases where two structures had the same value of *d*.

Zero-and one-dimensional aggregates sustained by Sn(II)…π(arene) interactions

Chemical structure diagrams of the 23 tin(II) molecules featuring zero- (**1**–**17**[24-34]) and one- (**18**–**23**[35-40]) dimensional aggregates sustained by Sn(lp)···π(arene) interactions are given in Fig. 3. Interesting, this number is greater than the number of structures, *i.e*. 22, included in the first systematic evaluation of M(lp)···π(arene) interactions, namely in tin(II) compounds.[6] Data for the 23 structures are given in Table 1. The following is an overview of the key structural motifs observed, with the aggregates illustrated in Fig. 4.

In common with most of the other elements covered in this survey, the most frequently observed aggregate is one where two mononuclear molecules are related about a centre of inversion and are connected by a pair of Sn(lp)···π(arene) interactions, as illustrated in Fig. 4a for **2**.[25] This motif, motif **0_I**, is adopted by **1**–**7**. In **4**,[27] for which two molecules comprise the crystallographic asymmetric unit, only one of these form Sn(lp)···π(arene) interactions. Essentially the same supramolecular **0_I** motif is found in the structures of each of binuclear **8**–**15**, illustrated in Fig. 4b by **15**;[24] in **13**,[24] only one of the two independent binuclear molecules associates in this fashion. The aggregate in **10**[24] is worthy of special mention as in addition to forming the Sn(lp)···π(arene) interactions to form the **0_I** dimer, each of the two remaining tin(II) centres form a Sn(lp)···π(arene) interaction to a solvent toluene molecule, Fig. 4c. In trinuclear **16**,[34] two independent molecules comprise the asymmetric unit and these associate *via* a single Sn(lp)···π(arene) interaction as shown in Fig. 4d; this is labelled as motif **0_II**. The molecule in **17**,[24] is a centrosymmetric tetranuclear species. In the crystal, centrosymmetrically related, tetranuclear molecules self-associate about a centre of inversion to generate motif **0_I**, Fig. 4e.

The remaining tin(II) structures self-associate into supramolecular chains of differing topology, adopting motif **1_I**. In mononuclear **18**,[35] linear supramolecular chains arise from a single donor and a single acceptor interaction per molecule, Fig. 4f. A similar situation

pertains for **19**[36] but the resulting topology is zigzag, Fig. 4g. In each of mononuclear **20**,[37] Fig. 4h, **21**[38] and **22**[39] similar chains are observed but, with helical topologies. In binuclear **23**,[40] only one of the independent tin(II) atoms forms Sn(lp)···π(arene) interactions, leading to a helical chain, **1_I**.

Zero-and one-dimensional aggregates sustained by Pb(II)…π(arene) interactions

Since the original review documenting the occurrence of Pb(lp)···π(arene) interactions,[7] another nine structures, **24-32**,[41-47] have appeared in the crystallographic literature having these structure-directing contacts, Fig. 5 and Table 1. Three of the structures adopt centrosymmetric dimeric motif **0_I**, with that found in **26**[43] illustrated in Fig. 6a. Two of the dimeric aggregates are sustained by a single Pb(lp)···π(arene) interaction only, thereby adopt motif **0_II**: that found in **27**[44] is shown in Fig. 6b.

Supramolecular chains are found in the crystal structures of the remaining four lead(II) compounds. A linear chain is found for **29**,[43] Fig. 6c, motif **1_I**. Each of **30**[45] and **31**[46] features a centrosymmetric, binuclear molecule. In the molecular packing each of the lead(II) atoms forms a Pb(lp)···π(arene) interaction so that each molecule participates in two donor and two acceptor interactions. The topology of the resulting chain is linear in each case, adopting motif **1_II**, and that found in **30** is shown in Fig. 6d. A non-symmetric, binuclear molecule is found in **32**[47] but each lead(II) atom participates in a Pb(lp)···π(arene) interaction so that a supramolecular chain ensures, with a helical topology. The new motif, *i.e.* **1_III**, is illustrated in Fig. 6e.

One-and two-dimensional aggregates sustained by Tl(I)…π(arene) interactions

Only three new thallium(I) structures, **33-35**,[48-50] Fig. 7 and Table 2, have appeared since the publication of the most recent review of M(lp)···π(arene) interactions, *i.e.* those involving

thallium(I).[8] Actually, there were a good number of "hits" but manual inspection revealed that the Tl(lp)···π(arene) interactions were cooperating with other supramolecular synthons, most commonly with Tl···O secondary bonding or conventional hydrogen bonding. Two of the crystal structures, **33**[48] and **34**,[49] feature motif **1_I**, *i.e*. helical supramolecular chains with that in the latter illustrated in Fig. 8a. A rare example of a two-dimensional architecture sustained by M(lp)···π(arene) interactions is found in the structure of **35**.[50] Compound **35** comprises centrosymmetric, binuclear molecules with each thallium(I) centre participating in Tl(lp)···π(arene) interactions. As these extend laterally, a layer ensures which has a flat topology as shown in Fig. 8b. This is classified as motif **2_I**.

One-and two-dimensional aggregates sustained by As(III)…π(arene) interactions

Even though there are only six new arsenic(III) structures with As(lp)···π(arene) interactions, **36**-**41**,[51-55] reported since the earlier review,[9] a rich diversity of supramolecular aggregation patterns in one- and two-dimensions are apparent, Fig. 9 and Table 3. A linear supramolecular chain sustained by As(lp)···π(arene) interactions is found in the crystal structure of **36**[51] These, motif **1_I**, are connected into tapes by conventional hydrogen bonding interactions *via* centrosymmetric, eight-membered {…HOC=O}$_2$ synthons, Fig. 10a. Linear chains (motif **1_I**) are also found in the structure of **37**.[52] As illustrated in Fig. 10b, putative secondary As···S and As···N can be envisaged along the direction of the chain but, these do not form as the As(lp)···π(arene) interactions predominate. In the crystal structure of **38**,[53] Fig. 10c, helical chains are formed; motif **1_I**. A tubular topology is found in the structure **39**,[54] and in isostructural **40**.[54] Aesthetically, these are most attractive aggregates as the tubes possess crystallographic 6_5 symmetry as highlighted in the end-on view of Fig. 10d. Unlike the previous structures in this category, the molecule in **41**[55] is binuclear and disposed

abut a centre of inversion. The central phenyl ring participates in two As(lp)···π(arene) interactions so that a flat layer (motif **2_I**) is formed as illustrated in Fig. 10e.

Zero-and one-dimensional aggregates sustained by Sb(III)···π(arene) interactions

Of the eight new antimony(III)-containing structures having structure-directing Sb(lp)···π(arene) interactions, **42**-**49**,[56-62] Fig. 11 and Table 3, and which have appeared since a systematic review of this phenomenon, four, **42**–**45**, feature zero-dimensional aggregation leading to motif **0_I**. An exemplar, namely **45**[59] is shown in Fig. 12a. Linear, supramolecular chains with mirror symmetry, are found in mononuclear **46**,[60] Fig. 12b and **47**.[60] The remaining two molecules also self-associate into motif **1_I** and give rise to helical chains, illustrated in the case of **48**[61] in Fig. 12c.

Zero-and one-dimensional aggregates sustained by Bi(III)···π(arene) interactions

At least 22 bismuth(III) structures featuring Bi(III)···π(arene) interactions have been published since a review of this phenomenon appeared in 2013,[10] **50**-**71**,[56, 63-78] Fig. 13 and Table 3. Of these, 13 adopt dimeric motif **0_I** as exemplified for the centrosymmetric aggregates in Fig. 14a for mononuclear **53**[64] and binuclear **61**,[70] Fig. 14b. The dimeric aggregate found in **62**,[71] Fig. 14c, is of interest from at least two perspectives. Firstly, this is a rare example of an aggregate of motif **0_I** lacking crystallographic symmetry. Also, **62** has a polymorph in the literature[79] which also self-associates *via* Bi(III)···π(arene) interactions [*d* = 3.76 Å, θ = 11.0º] but to form a linear supramolecular chain, *i.e.* motif **1_I**. Indeed, linear chains are found in several structures, Table 3, with that found in **63**[72] shown in Fig. 14d. Compound **64**[73] is noteworthy as each of the four independent molecules comprising the asymmetric unit forms Bi(III)···π(arene) interactions, with pairs of molecules associating to generate chains with linear topologies. There is an example of a zigzag chain, *i.e.* **66**,[74] Fig.

14e, and three helical chains, *e.g.* **68**,[76] Fig. 14f. In **67**,[75] each of the crystallographically independent molecules self-associates to form the helical chain. Finally, both independent bismuth(III) atoms in two binuclear molecules, **70**[78] and **71**,[78] Fig. 14g, form Bi(III)···π(arene) interactions leading to chains with a stepped topology, motif **1_IV**.

Zero-dimensional aggregates sustained by Se(II)···π(arene) interactions

With 52 structures featuring Se(II)···π(arene) interactions, **72**-**123**,[80-123] and one with a Se(IV)···π(arene) interaction, **124**,[124] selenium is the most significant contributor to the structures included in this survey, providing about one-third of the examples. There are 23 examples where Se(II)···π(arene) interactions lead to zero-dimensional motifs, Fig. 15 and Table 4. Compounds **72**–**84** feature the common, dimeric motif involving two mononuclear molecules, **0_I**, as exemplified for **74**[82] in Fig. 16a. The exceptional dimeric aggregate is found for **76**[84] where, rather than being centrosymmetric, the aggregate is located about a 2-fold axis, Fig. 16b. The binuclear molecules **85**–**89** are also zero-dimensional. While each of **85**[93] and **86**[94] employ a single selenium(II) to form the centrosymmetric dimer, in **87**,[95] where two independent molecules comprise the asymmetric unit, association into the dimer is *via* a single Se(II)···π(arene) interaction leading to motif **0_II**, Fig. 16c. Variations are found for **88**[96] and **89**.[97] In **88**,[96] Fig. 16d, with two independent molecules, both selenium(II) centres of one molecule associate *via* Se(II)···π(arene) interactions to the two rings of the second molecule. This is designated as motif **0_III**. In **89**,[97] both selenoether atoms of the macrocycle associate with another molecule about a centre of inversion, Fig.16e, so there are now four Se(II)···π(arene) interaction sustaining the dimer aggregate, motif **0_IV**. In tetranuclear **90**,[98] a centrosymmetric aggregate arises as a result of Se(II)···π(arene) interactions involving the selenoether atoms rather than the phosphorous selenide atoms, Fig. 16f. This observation is consistent with the previous systematic analysis of selenium

structures that suggested a preferential participation of selenoether- over selenide-selenium(II) in Se(II)···π(arene) interactions when there was a competition between the two.[11] Each of tetranuclear **91**,[98] **92**[99] and **93**,[100] Fig. 16g, associate about a centre of symmetry to form the **0_I** motif. A new motif, **0_V**, is found in the crystal structure of **94**.[85] Here, where two independent molecules comprise the asymmetric unit, one self-associates about a centre of inversion to form an aggregate akin to motif **0_I**. Associated with this are two molecules of the second independent molecule, each by a single Se(II)···π(arene) interaction, resulting in a four-molecule aggregate stabilised by four Se(II)···π(arene) interactions as shown in Fig. 16h.

One-dimensional aggregates sustained by Se(II)···π(arene) interactions

There are more one-dimensional aggregates sustained by Se(II)···π(arene) interactions than zero-dimensional aggregates, *i.e.* 29 *vs* 23. Chemical diagrams are given in Fig. 17 and data included in Table 4. The common supramolecular chains sustained by single Se(II)···π(arene) interactions are found, *i.e.* motif **1_I**. Thus, linear (**95**–**103**), zigzag (**104**–**109**) and helical (**110**–**114**) topologies are observed. Exemplars of these are shown in Figs 18a-c for **99**,[103] **105**[108] and **114**,[115] respectively. Binuclear molecules **115**–**118** employ a single selenium atom only to form linear supramolecular chains as illustrated for **117**[118] in Fig. 18d, and a zigzag chain is formed in the same way in the crystal structure of **119**,[120] Fig. 18e. Binuclear molecules **120**[121] and **121**,[82] Fig. 17f, utilise both selenium atoms to form linear chains and are designated as motif **1_II**. A new motif, *i.e.* **1_V**, arises in the crystal structure of **122**.[122] Here, binuclear molecules with 2-fold symmetry, self-associate about centres of inversion to form twisted chains, Fig. 18g. The final aggregation pattern to be described in this section involves an octanuclear molecule situated about a centre of

inversion, *i.e*. **123**.[123] These associate with translationally related molecules to generate a linear chain, motif **1_I**, Fig. 18h.

One-dimensional aggregate sustained by Se(IV)···π(arene) interactions

There is a sole example of a structure featuring Se(IV)···π(arene) interactions, namely that of **124**,[124] Fig. 19 and Table 4. In the crystal, molecules assemble into zigzag supramolecular chains *via* a single Se(IV)···π(arene) interaction per molecule, Fig. 20.

Zero-and one-dimensional aggregates sustained by Te(II)···π(arene) interactions

Chemical diagrams for tellurium(II) compounds described herein, **125-151**,[82, 125-138] forming Te(II)···π(arene) interactions are given in Fig. 21 and geometric data collated in Table 5. The mononuclear tellurium(II) compounds **125**–**127** adopt motif **0_I** with **127**[127] being notable as the molecules are not related over a centre of inversion, rather the two independent molecules comprising the asymmetric unit are connected by two Te(II)···π(arene) interactions, Fig. 22a. A large number of binuclear tellurium(II) compounds, **128**–**138** associate about a centre of inversion with only one of the independent tellurium(II) centres forming the Te(II)···π(arene) interaction. These are also designated as motif **0_I** and the aggregate found in **134**[128] is illustrated in Fig. 22b.

The remaining aggregates sustained by Te(II)···π(arene) interactions are one-dimensional. Mononuclear **139**–**144** self-assemble into linear chains *via* one Te(II)···π(arene) interaction per molecule. All of these are classified as motif **1_I** and are exemplified in Fig. 22c for **140**.[126] In the same manner, zigzag supramolecular chains are found in each of **145**[132] and **146**,[133] with the latter illustrated in Fig. 22d. Further representatives of motif **1_I** are found in the helical chains adopted by **147**[134] and **148**,[135] Fig. 22e. Only one of the tellurium(II) centres in binuclear **149**[136] forms Te(II)···π(arene) interactions to generate a

linear chain, Fig. 22f. A similar situation pertains for **150**[137] where the telluroether- rather than the telluride-tellurium(II) atom forms the interaction, leading to a zigzag chain, Fig. 22g. The final structure in this category is tetranuclear **151**,[138] which has 2-fold symmetry. Two tellurium(II) atoms per molecule participate in Te(II)···π(arene) interactions leading to a linear chain, Fig. 22h.

Zero-and one-dimensional aggregates sustained by Te(IV)···π(arene) interactions

There are six tellurium(IV) structures forming Te(IV)···π(arene) interactions, *i.e.* mononuclear **152-157**;[82, 139-142] see Fig. 23 for chemical diagrams and Table 5 for data. Two structures adopt motif **0_I**, being disposed about a centre of inversion in each case; **153**[140] is shown in Fig. 24a. The remaining structures each aggregate into a zigzag supramolecular chain sustained by a single Te(IV)···π(arene) interaction per molecule, *i.e.* motif **1_I**. Compound **155**[141] serves as an example, being illustrated in Fig. 24b.

Inspiration from biology

As highlighted in the Introduction, interest in element(lp)···π(aromatic ring) interactions was garnered from the apparent role of an oxygen(lp)···π(aromatic ring) contact is stabilising the conformation of the left-handed Z-DNA duplex.[1] As illustrated in Fig. 25, the participating oxygen atom is a cytidine-sugar-O atom and the π-system is a six-membered pyrimidinyl ring of a guanine residue; Figs 25-27 were drawn with DSVisualizer™ [143] using data extracted from the Protein Data Bank (PDB).[144] The presence of heavy element(lp)···π(aromatic ring) interactions in macromolecular structures has been mentioned to in some of the earlier reviews on this topic.[10-12] In keeping with the theme of the present update, two examples of

such interactions involving neutral molecules incorporating element(lp) interacting with a protein and an enzyme are presented.

In the first exemplar, the interaction of the cyclic hexapeptide inhibitor, cyclic tris-valinyl-selenazole (QZ-Val), Fig. 26a, with the membrane transporter protein P-glycoprotein (P-gp), which has pharmacological relevance, being a transporter of drug metabolites across cell membranes, has been described recently.[145] As seen from Figs 26b and c, some of the selenium(II) atoms of QZ-Val are linked to P-gp *via* selenium(lp)···π(arene) contacts in this co-crystal.

The second exemplar, an enzyme-inhibitor complex, is remarkable from several perspectives and is discussed here even though the π-system is not an arene ring. The study in question revealed the interactions of analogues of sarcosine, Fig. 27a, with the enzyme, sarcosine oxidase, specifically the active site, the covalently bound flavin adenine dinucleotide (FAD).[146] The analogues were those where the NH group of sarcosine was replaced by species such as X = methylene, selenium(II), *etc*. Crucially, the authors of this paper, published in 2000, concluded that the binding affinity, which followed the order CH_2 < O < S < Se < Te, was related to the ability of X to form X(lp)…π interactions in the receptor site. This notion is entirely consistent with the concepts explaining the formation of X(lp)…π interactions as outlined in the *Introduction*. Crystallography on the co-crystals reveals the positioning of tellurium(II), Fig. 27b, and selenium(II) over the rings,[146] akin to that seen in molecular compounds. Clearly, there is enormous scope for further study designed to unravel the nature and relative importance of element(lp)…π interactions in macromolecular systems.

Overview

The previous sections have shown that element(lp)…π interactions provide definitive points of contact between molecules leading to clearly recognisable supramolecular aggregates. As the specified element(lp)…π interaction occurs in isolation of other recognisable supramolecular synthons, these may be termed structure-directing. The foregoing notwithstanding, several interrelated questions arise as to their prevalence, their strength and, crucially, their relevance to crystal engineering endeavours.

Of the heavier main group elements covered herein, the maximum adoption of independent element(lp)…π interactions occur in thallium(I) structures, at about 14%. Bismuth(III) structures are 9% likely to feature analogous interactions with the other elements having lower probabilities, down to a minimum of 2-3% for tin(II) and lead(II) compounds. To put this in context, the well-recognised eight-membered $\{\ldots HOCO\}_2$ synthon occurs in just one-third of structures where they can potentially form owing to competing supramolecular interactions.[147] However, the percentage adoption of element(lp)…π interactions in molecular packing will be higher than indicated above as these can operate in cooperation with other synthons but, as indicated above, these structures were excluded from the present survey.

The energy of stabilisation imparted by element(lp)…π interactions is small and likely to be less than 10 kJ mol^{-1}.[1, 14, 148] In keeping with their weak nature and as anticipated for weak interactions, no correlation between *d* and θ exists[6-12] as occurs for conventional hydrogen bonding interactions. This lack of correlation is related to the great diversity of the chemical composition of the molecules and their inherent weak nature.[12a, 149]

Conclusions

The observation of element(lp)…π interactions date back over a Century in the form of Menschutkin complexes of which the $SbCl_3$ complex with benzene is the prominent

example.[150] Over the past decade, data mining investigations have shown that analogous element(lp)…π interactions are pivotal in assembling molecules into, usually, zero- and one-dimensional aggregates, and less commonly into two- and three-dimensional architectures.[5-12] While inherently weak, these interactions play a role in stabilising crystal structures, often being structure-directing and any thorough analysis of supramolecular association should include a search for element(lp)…π interactions involving both light- and heavier-element species. While the exploitation of element(lp)…π interactions in deliberate crystal engineering endeavours is in its infancy, the very recent reports of interacting halogenated solvent with substituted triazine rings *via* element(lp)…π interactions[151] and the direct spectroscopic observation of element(lp)…π interactions in substituent formates[152] suggest that element(lp)…π interactions may have a role in arranging molecules in the condensed phase.

Acknowledgements

The Brazilian agencies National Council for Scientific and Technological Development (CNPq-306121/2013-2 to IC, 305626/2013-2 to JZS) and Brazilian Federal Foundation for Support and Evaluation of Graduate Education (CAPES) are acknowledged for financial support.

References

1 M. Egli and R. V. Gessner, *Proc. Natl. Acad. Sci. U. S. A.*, 1995, **92**, 180; M. Egli and S. Sarkhel, *Acc. Chem. Res*., 2007, **40**, 197.

2 A. Jain, V. Ramanathan and R. Sankararamakrishnan, *Protein Sci*., 2009, **18**, 595.

3 T. J. Mooibroek, P. Gamez and J. Reedijk, *CrystEngComm*, 2008, **10**, 1501.

4 J. Zukerman-Schpector and I. Haiduc, *CrystEngComm*, 2002, **4**, 178.

5 J. Zukerman-Schpector, I. Haiduc and E.R.T. Tiekink, *Chem. Commun*., 2011, **47**, 12682; J. Zukerman-Schpector, I. Haiduc and E. R. T. Tiekink, *Adv. Organomet. Chem*., 2012, **60**, 49; J. Zukerman-Schpector and E. R. T. Tiekink, *CrystEngComm*, 2014, **16**, 6398.

6 I. Haiduc, E. R. T. Tiekink and J. Zukerman-Schpector, in Tin Chemistry Fundamentals, Frontiers, and Applications, ed. A. G. Davies, M. Gielen, K. H. Pannell and E. R. T. Tiekink, John Wiley & Sons Ltd., Chichester, 2008, p. 392.

7 E. R. T. Tiekink and J. Zukerman-Schpector, *Aust. J. Chem.*, 2010, **63**, 535.

8 I. Caracelli, I. Haiduc, J. Zukerman-Schpector and E. R. T. Tiekink, *Coord. Chem. Rev.*, 2014, **281**, 50.

9 J. Zukerman-Schpector, A. Otero-dela-Roza, V. Luaña and E. R. T. Tiekink, *Chem. Commun.*, 2011, **47**, 7608.

10 I. Caracelli, I. Haiduc, J. Zukerman-Schpector and E. R. T. Tiekink, *Coord. Chem. Rev.*, 2013, **257**, 2863.

11 (a) I. Caracelli, J. Zukerman-Schpector and E. R. T. Tiekink, *Coord. Chem. Rev.*, 2012, **256**, 412; (b) I. Caracell, I. Haiduc, J. Zukerman-Schpector and E. R. T. Tiekink, in The Chemistry of Organic Selenium and Tellurium Compounds, ed. Z. Rappoport, John Wiley & Sons, Ltd, Chichester, 2013, vol. 4, p. 973.

12 (a) E. R. T. Tiekink and J. Zukerman-Schpector, *CrystEngComm*, 2009, **11**, 2701; (b) I. Haiduc, E. R. T. Tiekink and J. Zukerman-Schpector, in *The Importance of Pi-Interactions in Crystal Engineering*, eds E. R. T. Tiekink and J. Zukerman-Schpector, John Wiley & Sons, Ltd, Chichester, 2012, pp. 301.

13 I. Haiduc and J.J. Zuckerman, *Basic Organometallic Chemistry*, Walter de Gruyter, Berlin, New York, 1985.

14 G. A. DiLabio and E. R. Johnson, *J. Am. Chem. Soc*., 2007, **129**, 6199; H.-Y. Zhuo, Q.-Z. Li, W.-Z. Li, and J. B. Cheng, *Phys. Chem. Chem. Phys*., 2014, **16**, 159; A. Otero-de-la-Roza, V. Luaña, E. R. T. Tiekink and J. Zukerman-Schpector, *J. Chem. Theory Comput*. 2014, **10**, 5010; C. Murcia-García, A. Bauzá, A. Frontera and R. Streubel, *CrystEngComm*, 2015, **17**, 6736; T. Montoro, G. Tardajos, A. Guerrero, M. del Rosario Torres, C. Salgado, I. Fernández and J. Osío Barcina, *Org. Biomol. Chem*., 2015, **13**, 6194.

15 G. Cavallo, P. Metrangolo, R. Milani, T. Pilati, A. Priimagi, G. Resnati and G. Terraneo, *Chem. Rev*., 2016, **116**, 2478.

16 G. R. Desiraju, *Angew. Chem. Int. Edn*., 2007, **46**, 8342.

17 C. R. Groom, I. J. Bruno, M. P. Lightfoot and S. C. Ward, *Acta Crystallogr., Sect. B: Struct. Sci., Cryst. Eng. & Mat*., 2016, **72**, 171.

18 I. J. Bruno, J. C. Cole, P. R. Edgington, M. Kessler, C. F. Macrae, P. McCabe, J. Pearson and R. Taylor, *Acta Crystallogr., Sect. B: Struct. Sci*., 2002, **58**, 389.

19 C. Janiak, *J. Chem. Soc., Dalton Trans*., 2000, 3885.

20 D. Schollmeyer, O.V. Shishkin, T. Rühl and M.O. Vysotsky, *CrystEngComm*, 2008, **10**, 715; O.V. Shishkin, *Chem. Phys. Lett*., 2008, **458**, 96.

21 S. Sewpersad and W. E. Van Zyl, *Acta Crystallogr., Sect. E: Struct. Rep. Online*, 2012, **68**, m1502.

22 DIAMOND, Visual Crystal Structure Information System, Version 3.1, CRYSTAL IMPACT, Postfach 1251, D-53002 Bonn, Germany, 2006.

23 A. L. Spek, *J. Appl. Crystallogr*., 2003, **36**, 7.

24 T. J. Boyle, T. Q. Doan, L. A. M. Steele, C. Apblett, S. M. Hoppe, K. Hawthorne, R. M. Kalinich and W. M. Sigmund, *Dalton Trans*., 2012, **41**, 9349.

25 S. L. Choong, W. D. Woodul, C. Schenk, A. Stasch, A. F. Richards and C. Jones, *Organometallics*, 2011, **30**, 5543.

26 A. Akkari, J. J. Byrne, I. Saur, G. Rima, H. Gornitzka and J. Barrau, *J. Organomet. Chem.*, 2001, **622**, 190.

27 M. Ibarra-Rodriguez, V. M. Jimenez-Perez, B. M. Munoz-Flores, N. Waksman, R. Ramirez, M. Sanchez and I. F. Hernandez-Ahuactzi, *Arab. J. Chem.*, 2015, doi:10.1016/j.arabjc.2015.08.030.

28 H.-M. Kao, S.-M. Ho, I-C. Chen, P.-C. Kuo, C.-Y. Lin, C.-Y. Tu, C.-H. Hu, J.-H. Huang and G.-H. Lee, *Inorg. Chim. Acta*, 2008, **361**, 2792.

29 R. Olejnik, Z. Padelkova, R. Mundil, J. Merna and A. Ruzicka, *Appl. Organomet. Chem*., 2014, **28**, 405.

30 A. Jana, H. W. Roesky, C. Schulzke, A. Doring, T. Beck, A. Pal and R. Herbst-Irmer, *Inorg. Chem*. 2009, **48**, 193.

31 F. E. Hahn, A. V. Zabula, T. Pape, A. Hepp, R. Tonner, R. Haunschild and G. Frenking, *Chem.-Eur. J*., 2008, **14**, 10716.

32 S. Krupski, C. S. to Brinke, H. Koppetz, A. Hepp and F. E. Hahn, *Organometallics*, 2015, **34**, 2624.

33 M. Ibarra-Rodriguez, H. V. R. Dias, V. M. Jimenez-Perez, B. M. Munoz-Flores, A. Flores-Parra and S. Sanchez, *Z. Anorg. Allg. Chem*. 2012, **638**, 1486.

34 A.V. Zabula, T. Pape, F. Hupka, A. Hepp and F. E. Hahn, *Organometallics*, **28**, 4221.

35 M. El Ezzi, R. Lenk, D. Madec, J.-M. Sotiropoulos, S. Mallet-Ladeira and A. Castel, *Angew. Chem., Int. Ed*. 2015, **54**, 805.

36 S. Krupski, R. Pöttgen, I. Schellenberg and F. E. Hahn, *Dalton Trans*. 2014, **43**, 173.

37 J. V. Dickschat, S. Urban, T. Pape, F. Glorius and F. E. Hahn, *Dalton Trans*., 2010, **39**, 11519.

38 M. Huang, M. M. Kireenko, E. Kh Lermontova, A. V. Churakov, Y. F. Oprunenko, K. V. Zaitsev, D. Sorokin, K. Harms, J. Sundermeyer, G. S. Zaitseva and S. S. Karlov, *Z. Anorg. Allg. Chem*., 2013, **639**, 502.

39 R. Selvaraju, K. Panchanatheswaran and V. Parthasarathi, *Acta Crystallogr., Sect. C: Cryst. Struct. Commun.*, 1998, **54**, 905.

40 W. A. Merrill, J. Steiner, A. Betzer, I. Nowik, R. Herber and P. P. Power, *Dalton Trans*. 2008, 5905.

41 B. A. Iglesias, D. F. Back, M. Horner, E. R. Crespan and F. Broch, *J. Organomet. Chem*., 2014, **752**, 12.

42 E. C. Y. Tam, M. P. Coles, J. D. Smith and J. R. Fulton, *Polyhedron*, 2015, **85**, 284.

43 A. Jana, S. P. Sarish, H. W. Roesky, C. Schulzke, A. Doring and M. John, *Organometallics*, 2009, **28**, 2563.

44 C. Jones, A. Sidiropoulos, N. Holzmann, G. Frenking and A. Stasch, *Chem. Commun.*, 2012, **48**, 9855.

45 G. Mohammadnezhad, M. M. Amini and V. Langer, *Acta Crystallogr., Sect. C: Cryst. Struct. Commun*., 2010, **66**, m44.

46 G. Mohammadnezhad Sh., M. M. Amini and S. W. Ng, *Acta Crystallogr., Sect. E: Struct. Rep. Online*, 2009, **65**, m261.

47 E. Lopez-Torres and M. A. Mendiola, *Dalton Trans*., 2009, 7639.

48 T. J. Boyle, C. A. Zechmann, T. M. Alam, M. A. Rodriguez, C. A. Hijar and B. L. Scott, *Inorg. Chem*., 2002, **41**, 946

49 Y. Rong, J. H. Palmer and G. Parkin, *Dalton Trans*., 2014, **43**, 1397

50 G. Gomathi, S. Thirumaran and S. Ciattini, *Polyhedron*, 2015, **102**, 424.

51 I. Yu. Ilyin, N. A. Pushkarevsky, N. V. Kuratieva, D. Yu. Naumov and S. N. Konchenko, *Acta Crystallogr., Sect. C: Cryst. Struct. Commun.* 2012, **68**, m323.

52 V. Matuska, A. M. Z. Slawin and J. D. Woollins, *Inorg. Chem*., 2010, **49**, 3064.

53 S. Maheshwari, K. Bundela and K. G. Ojha, *J. Coord. Chem*. 2014, **67**, 1088.

54 N. L. Kilah and S. B. Wild, *Organometallics*, 2012, **31**, 2658.

55 V. M. Cangelosi, T. G. Carter, L. N. Zakharov and D. W. Johnson, *Chem. Commun*., 2009, 5606.

56 N. Tan, Y. Chen, S.-F. Yin, R. Qiu, Y. Zhou and C. T. Au, *Dalton Trans*., 2013, **42**, 9476.

57 L. Dostál, R. Jambor, A. Růžička, R. Jirásko, A. Lyčka, J. Beckmann and S. Ketkov, *Inorg. Chem*., 2015, **54**, 6010.

58 Y. Chen, K. Yu, N.-Y. Tan, R.-H. Qiu, W. Liu, N.-L. Luo, L. Tong, C.-T. Au, Z.-Q. Luo and S.-F. Yin, Eur. *J. Med. Chem*., 2014, **79**, 391.

59 E. Hupf, E. Lork, S. Mebs, L. Chęcińska and J. Beckmann, *Organometallics*, 2014, **33**, 7247.

60 S. L. Benjamin, W. Levason, G. Reid and R. P. Warr, *Organometallics*, 2012, **31**, 1025.

61 A. Toma, C. I. Rat, A. Silvestru, T. Ruffer, H. Lang and M. Mehring, *J. Organomet. Chem*., 2013, **745**, 71.

62 J. G. Alvarado-Rodriguez, S. Gonzalez-Montiel and N. Andrade-Lopez, *Main Group Met. Chem*., 2013, **36**, 21.

63 N. Tan, Y. Chen, Y. Zhou, C.-T. Au, S.-F. Yin, *ChemPlusChem*, 2013, **78**, 1363.

64 A. Luqman, V. L. Blair, R. Brammananth, P. K. Crellin, R. L. Coppel, L. Kedzierski and P. C. Andrews, *Eur. J. Inorg. Chem.*, 2015, 725.

65 R. Qiu, Z. Meng, S. Yin, X. Song, N. Tan, Y. Zhou, K. Yu, X. Xu, S. Luo, C.-T. Au and W.-Y. Wong, *ChemPlusChem*, 2012, **77**, 404.

66 B. T. Worrell, S. P. Ellery and V. V. Fokin, *Angew. Chem., Int. Ed*., 2013, **52**, 13037.

67 M. G. Nema, H. J. Breunig, A. Soran and C. Silvestru, *J. Organomet. Chem*., 2012, **705**, 23.

68 A. Toma, C. I. Rat, A. Silvestru, T. Ruffer, H. Lang, and M. Mehring, *J. Organomet. Chem*., 2013, **745**, 71.

69 A. Schulz and A. Villinger, *Organometallics*, 2011, **30**, 284.

70 I. Kumar, P. Bhattacharya and K. H. Whitmire, *J. Organomet. Chem*., 2015, **794**, 153.

71 H.-G. Stammler and B. Neumann, Private Communication to the CSD (BITRPH11).

72 S. L. Benjamin, W. Levason, G. Reid, M. C. Rogers and R. P. Warr, *J. Organomet. Chem.*, 2012, **708**, 106.

73 A. Toma, C. I. Rat, A. Silvestru, T. Ruffer, H. Lang and M. Mehring, *J. Organomet. Chem.*, 2016, **806**, 5.

74 X.-W. Zhang and T. Fan, *Acta Crystallogr., Sect. E: Struct. Rep. Online*, 2011, **67**, m875.

75 B. Nekoueishahraki, P. P. Samuel, H. W. Roesky, D. Stern, J. Matussek, D. Stalke, *Cryst. Growth Des.*, 2012, **31**, 6697.

76 G. G. Briand, A. Decken, N. M. Hunter, G. M. Lee, J. A. Melanson and E. M. Owen, *Polyhedron*, 2012, **31**, 796.

77 M. L. N. Rao and R. J. Dhanorkar, *RSC Advances*, 2016, **6**, 1012.

78 I. Kumar, P. Bhattacharya and K. H. Whitmire, *J. Organomet. Chem*., 2015, **794**, 153.

79 P. G. Jones, A. Blaschette, D. Henschel and A. Weitze, *Z. Kristallogr*., 1995, **210**, 377.

80 P. Arsenyan, E. Paegle, S. Belyakov, I. Shestakova, E. Jaschenko, I. Domracheva and J. Popelis, *Eur. J. Med. Chem*., 2011, **46**, 3434.

81 K. Srivastava, T. Chakraborty, H. B. Singh and R. J. Butcher, *Dalton Trans*., 2011, **40**, 4489.

82 L. K. Aschenbach, F. R. Knight, R. A. M. Randall, D. B. Cordes, A. Baggott, M. Buhl, A. M. Z. Slawin and J. D. Woollins, *Dalton Trans*., 2012, **41**, 3141.

83 B. Godoi, A. Sperança, C. A. Bruning, D. F. Back, P. H. Menezes, C. W. Nogueira and G. Zeni, *Adv. Synth. Catal*., 2011, **353**, 2042.

84 A. Bedi, S. Debnath, H. S. Chandak and S. S. Zade, *RSC Advances*, 2014, **4**, 35653.

85 S. Mondal, M. Konda, B. Kauffmann, M. K. Manna and A. K. Das, *Cryst. Growth Des*., 2015, **15**, 5548.

86 J. A. Roehrs, R. P. Pistoia, D. F. Back and G. Zeni, *J. Org. Chem*., 2015, **80**, 12470.

87 D. B. Cordes, G. Hua, A. M. Z. Slawin and J. D. Woollins, *Acta Crystallogr., Sect. C: Cryst. Struct. Commun*., 2011, **67**, o509.

88 J. Muthukumaran, M. Nishandhini, S. Chitra, P. Manisankar, S. Bhattacharya, S. Muthusubramanian, R. Krishna and J. Jeyakanthan, *Acta Crystallogr., Sect. E: Struct. Rep. Online*, 2011, **67**, o1660.

89 V. P. Singh, H. B. Singh and R. J. Butcher, *Chem. Asian J.*, 2011, **6**, 1431.

90 J. Muthukumaran, M. Nachiappan, S. Chitra, P. Manisankar, S. Bhattacharya, S. Muthusubramanian, R. Krishna and J. Jeyakanthan, *Acta Crystallogr., Sect. E: Struct. Rep. Online*, 2011, **67**, o2010.

91 M. W. Stanford, F. R. Knight, K. S. A. Arachchige, P. S. Camacho, S. E. Ashbrook, M. Buhl, A. M. Z. Slawin and J. D, Woollins, *Dalton Trans*., 2014, **43**, 6548.

92 M. S. Afzal, J.-P. Pitteloud and D. Buccella, *Chem. Commun*., 2014, **50**, 11358.

93 P. Rakesh, H. B. Singh, J. P. Jasinski and J. A. Golen, *Dalton Trans*., 2014, **43**, 9431.

94 C. Figliola, L. Male, P. N. Horton, M. B. Pitak, S. J. Coles, S. L. Horswell and R. S. Grainger, *Organometallics*, 2014, **33**, 4449.

95 D. M. Freudendahl, M. Iwaoka and T. Wirth, *Eur. J. Org. Chem.*, 2010, pp. 3934.

96 C. G. M. Benson, C. M. Schofield, R. A. M. Randall, L. Wakefield, F. R. Knight, A. M. Z. Slawin and J. D. Woollins, *Eur. J. Inorg. Chem.*, 2013, pp. 427.

97 M. Masuda, C. Maeda and N. Yoshioka, *Org. Lett*., 2013, **15**, 578.

98 G. Hua, A. M. Z. Slawin, R. A. M. Randall, D. B. Cordes, L. Crawford, M. Buhl and J. D. Woollins, *Chem. Commun*., 2013, **49**, 2619.

99 X. Xiong, C.-L. Deng, B. F. Minaev, G. V. Baryshnikov, X.-S. Peng and H. N. C. Wong, *Chem. Asian J*., 2015, **10**, 969.

100 M. D. Milton, N. Kumar, S. S. Sokhi, S. Singh, M. Maheshwari, J. D. Singh, M. Asnani and R. J. Butcher, *Tetrahedron Lett*., 2004, **45**, 8941.

101 T. M. Klapotke, B. Krumm and M. Scherr, *Z. Anorg. Allg. Chem.*, 2010, **636**, 1955.

102 C. R. Cerqueira Jr, P. R. Olivato, D. N. S. Rodrigues, J. Zukerman-Schpector, E. R. T. Tiekink and M. D. Colle, *J. Mol. Struct*., 2015, **1084**, 190.

103 T. Murai, D. Nishi, S. Hayashi and W. Nakanishi, *Bull. Chem. Soc. Jpn*, 2014, **87**, 677.

104 S. J. Balkrishna, B. S. Bhakuni, D. Chopra and S. Kumar, *Org.Lett.*, 2010, **12**, 5394.

105 S. P. Thomas, K. Satheeshkumar, G. Mugesh and T. N. Guru Row, *Chem.-Eur. J.*, 2015, **21**, 6793.

106 K. Grenader, M. Kind, L. Silies, A. Peters, J. W. Bats, M. Bolte and A. Terfort, *J. Mol. Struct*., 2013, **1039**, 61.

107 G. Hua, J. Du, A. L. Fuller, K. S. A. Arachchige, D. B. Cordes, A. M. Z. Slawin, J. D. Woollins, *Synlett*, 2015, **26**, 839.

108 E. A. Popova, M. L. Petrov and A. G. Lyapunova, *Private Communication to the CSD* (QOVGAL).

109 A. Ishii, T. Annaka and N. Nakata, *Chem.-Eur. J.*, 2012, **18**, 6428.

110 P. Rakesh, H. B. Singh and R. J. Butcher, *Organometallics*, 2013, **32**, 7275.

111 G. Hua, J. Du, A. M. Z. Slawin and J. D. Woollins, *J. Org. Chem.*, 2014, **79**, 3876.

112 P. Sugumar, S. Sankari, P. Manisankar, V. Thiruselvam and M. N. Ponnuswamy, *Acta Crystallogr., Sect. E: Struct. Rep. Online*, 2013, **69**, o1239.

113 S. Sankari, P. Sugumar, T. Manisankar, S. Muthusubramanian and M. N. Ponnuswamy, *Acta Crystallogr., Sect. E: Struct. Rep. Online*, 2012, **68**, o447.

114 P. Sugumar, S. Sankari, P. Manisankar and M. N. Ponnuswamy, *Acta Crystallogr., Sect. E: Struct. Rep. Online*, 2012, **68**, o2347.

115 T. Murai, K. Yamaguchi, F. Hori and T. Maruyama, *J. Org. Chem.*, 2014, **79,** 4930.

116 N. A. Barnes, S. M. Godfrey, J. Hughes, R. Z. Khan, I. Mushtaq, R. T. A. Ollerenshaw, R. G. Pritchard and S. Sarwar, *Dalton Trans.*, 2013, **42**, 2735.

117 T. Kimura, T. Nakahodo, H. Fujihara and E. Suzuki, *Inorg. Chem.*, 2014, **53**, 4411.

118 A. Linden, Y. Zhou and H. Heimgartner, *Acta Crystallogr., Sect. C: Cryst. Struct. Chem.*, 2014, **70**, 482.

119 T. Mitamura, K. Iwata, A. Nomoto and A. Ogawa, *Org. Biomol. Chem.*, 2011, **9**, 3768.

120 K. Selvakumar, P. Shah, H. B. Singh and R. J. Butcher, *Chem.-Eur. J.*, 2011, **17**, 12741.

121 S. Panda, P. Kr. Dutta, G. Ramakrishna, C. M. Ready and S. S. Zade, *J. Organomet. Chem.*, 2012, **717**, 45.

122 E. M. Takaluoma, T. T. Takaluoma, R. Oilunkaniemi and R. S. Laitinen, *Z. Anorg. Allg. Chem.*, 2015, **641**, 772.

123 J. Thomas, L. Dobrzańska, L. Van Meervelt, M. A. Quevedo, K. Woźniak, M. Stachowicz, M. Smet, W. Maes and W. Dehaen, *Chem.-Eur. J.*, 2015, **22**, 979.

124 A. G. Makarov, T. D. Grayfer, A. Yu. Makarov, I. Yu. Bagryanskaya, V. G. Vasiliev and A. V. Zibarev, *Mendeleev Commun*., 2011, **21**, 320.

125 K. Srivastava, P. Shah, H. B. Singh and R. J. Butcher, *Organometallics*, 2011, **30**, 534.

126 B. Singh, A. K. S. Chauhan, R. C. Srivastava, A. Duthie and R. J. Butcher, *RSC Advances*, 2015, **5**, 58246.

127 F. A. Tsao, A. J. Lough and D. W. Stephan, *Chem. Commun.*, 2015, **51**, 4287.

128 F. R. Knight, L. M. Diamond, K. S. A. Arachchige, P. S. Camacho, R. A. M. Randall, S. E. Ashbrook, M. Buhl, A. M. Z. Slawin and J. D. Woollins, *Chem.-Eur. J*., 2015, **21**, 3613.

129 M. Buehl, F. R. Knight, A. Kristkova, I. M. Ondik, O. L. Malkina, R. A. M. Randall, A. M. Z. Slawin and J. D. Woollins, *Angew. Chem., Int. Ed*., 2013, **52**, 2495.

130 E. Faoro, G. M. de Oliveira, E. S. Lang and C. B. Pereira, *J. Organomet. Chem*., 2011, **696**, 2438.

131 T. Nakai, N. Nishino, S. Hayashi, M. Hashimoto and W. Nakanishi, *Dalton Trans*., 2012, **41**, 7485.

132 A. K. S. Chauhan, P. Singh, R. C. Srivastava, R. J. Butcher and A. Duthie, *J. Organomet. Chem.*, 2010, **695**, 2118.

133 T. Annaka, N. Nakata and A. Ishii, *Organometallics*, 2015, **34**, 1272.

134 S. Kawaguchi, T. Ohe, T. Shirai, A. Nomoto, M. Sonoda and A. Ogawa, *Organometallics*, 2010, **29**, 312.

135 N. Assadi, S. Cohen, S. Pogodin and I. Agranat, *Struct. Chem*., 2015, **26**, 319.

136 A. L. Fuller, L. A. S. Scott-Hayward, Y. Li, M. Buhl, A. M. Z. Slawin and J. D. Woollins, *J. Am. Chem. Soc*., 2010, **132**, 5799.

137 H. Sashida, M. Kaname, A. Nakayama, H. Suzuki and M. Minoura, *Tetrahedron*, 2010, **66**, 5149.

138 J. Beckmann and J. Bolsinger, *Z. Anorg. Allg. Chem*., 2011, **637**, 29.

139 R. Cargnelutti, E. S. Lang, G. M. de Oliveira and P. C. Piquini, *Polyhedron*, 2012, **39**, 106.

140 S. Ogawa, S. Ohwada, M. Yoshida and H. Muraoka, *Heteroat. Chem.*, 2011, 22, 586.

141 J. Beckmann, D. Dakternieks, A. Duthie, C. Mitchell and M. Schurmann, *Aust. J. Chem*., 2005, **58**, 119.

142 A. K. S. Chauhan, S. N. Bharti, R. C. Srivastava, R. J. Butcher and A. Duthie, *J. Organomet. Chem*., 2012, **708**, 75.

143 DSVisualizer^{TM} – Accelrys Software Inc., DiscoveryStudio Visualizer 3.0, http://accelrys.com/products/discovery-studio/visualization/

144 PDB Protein Data Bank: http//www.rcsb.org/pdb/home/home.do

145 P. Szewczyk, H. Tao, A. P. McGrath, M. Villaluz, S. D. Rees, S. C. Lee, R. Doshi, I. L. Urbatsch, Q. Zhang and G. Chang, *Acta Crystallogr., Sect. D: Biol. Crystallogr*., 2015, **71**, 732.

146 M. A. Wagner, P. Trickey, Z.-W. Chen, F. S. Mathews and M. S. Jorns, *Biochemistry*, 2000, **39**, 8813.

147 F. H. Allen, W. D. S. Motherwell, P. R. Raithby, G. P. Shields and R. Taylor, *New J. Chem*., 1999, **23**, 25.

148 A. Bauzá, D. Quiñonero, P. M. Deyà and A. Frontera, *Phys. Chem. Chem. Phys*., 2012, **14**, 14061; M. Mascal, A. Armstrong and M. D. Bartberger, *J. Am. Chem. Soc*.

2002, **124**, 6274; D. Kim, P. Tarakeshwar and K. S. Kim, *J. Phys. Chem. A*, 2004, **108**, 1250; B. W. Gung, Y. Zou, Z. Xu, J. C. Amicangelo, D. G. Irwin, S. Ma and H.-C. Zhou, *J. Org. Chem*., 2008, 73, 689.

149 J. D. Dunitz and R. Taylor, *Chem. Eur. J*., 1997, **3**, 89.

150 H. Schmidbaur and A. Schier, *Organometallics*, 2008, **27**, 2361; A. Schier, J. M. Wallis, G. Müller and H. Schmidbaur, *Angew. Chem. Int. Ed. Engl*., 1986, **25**, 757.

151 S. Mehrotra and R. Angamuthu, *CrystEngComm*, 2016, **18**, 4438.

152 S. K. Singh, K. K. Mishra, N. Sharma and A. Das, *Angew. Chem. Int. Edn*., 2016, **55**, 7801.

Table 1 Geometric parameters characterising Sn(lp)…π(arene) interactions in **1**–**23**, and Pb(lp)…π(arene) interactions in **24**–**32**

Compound	CSD ref. code	*d* (Å)	θ (º)	Motif	Ref.
Sn(II) structures					
Zero-dimensional aggregates					
1	HEBXOB01	3.47	4.5	**0_I**	24
2	QIVNUE01	3.62	11.5	**0_I**	25
3	QOXQID	3.76	11.2	**0_I**	26
4	ZUNYAK	3.80	17.5	**0_I**	27
5	OGAPES	3.85	8.0	**0_I**	28
6	ZOBGEE	3.86	12.5	**0_I**	29
7	YOMVAY	4.02	19.6	**0_I**	30
8	VAYTEW	3.25	7.6	**0_I**	24
9	TOMWIC	3.34	7.1	**0_I**	31
10	VAYTIA	3.36	10.8	**0_I**	24
		3.59	7.6 (solvent)		
11	BUHTIJ	3.37	7.2	**0_I**	32
12	BEMMOX	3.40	4.0	**0_I**	33
13	VAYRUK	3.44	8.9	**0_I**	24
14	VAYSIZ	3.68	5.7	**0_I**	24
15	VAYRIY	3.69	8.2	**0_I**	24
16	LUCZIT	3.58	11.3	**0_II**	34
17	VAYTAS	3.26	11.9	**0_I**	24
One-dimensional aggregates					

18	KOXCUX	3.71	11.6	**1_I** (linear)	35
19	LIJMOI	3.63	13.3	**1_I** (zigzag)	36
20	ULOLOX	3.44	8.9	**1_I** (helical)	37
21	NIDTOL	3.76	2.8	**1_I** (helical)	38
22	NUMWEX	4.00	16.6	**1_I** (helical)	39
23	BOKBOT	3.38	8.2	**1_I** (helical)	40
Pb(II) structures					
Zero-dimensional aggregates					
24	GISDET	3.47	4.3	**0_I**	41
25	DABCUH	3.49	11.6	**0_I**	42
26	HUGVUB	3.89	18.9	**0_I**	43
27	DAYVOQ	3.75	3.6	**0_II**	44
28	DUZRIB	3.75	12.1	**0_II**	42
One-dimensional aggregates					
29	HUGWEM	3.17	8.3	**1_I** (linear)	43
30	KUQFAE01	3.47	12.8	**1_II** (linear)	45
31	GOLMOK	3.91	17.3	**1_II** (linear)	46
32	TUMFAJ	3.34	8.3	**1_III** (helical)	47
		3.40	12.0		

Table 2 Geometric parameters characterising Tl(lp)…π(arene) interactions in **33**–**35**

Compound	CSD ref. code	*d* (Å)	θ (º)	Motif	Ref.
One-dimensional aggregates					
33	MIBZIG	3.06	6.8	**1_I** (helical)	48
34	DIPSAY	3.35	11.5	**1_I** (helical)	49
Two-dimensional aggregate					
35	QUQZIN	3.24	2.6	**2_I** flat	50

Table 3 Geometric parameters characterising As(lp)…π(arene) interactions in **36**–**41**, Sb(lp)…π(arene) interactions in **42**–**49** and Bi(lp)…π(arene) interactions in **50**–**71**

Compound	CSD ref. code	*d* (Å)	θ (º)	Motif	Ref.
As(III) structures					
One-dimensional aggregates					
36	FEFHOP	3.47	9.2	**1_I** (linear)	51
37	RUTXUA	3.48	6.9	**1_I** (linear)	52
38	DIYCOF	3.36	13.4	**1_I** (helical)	53
39	GETLUO	3.70	12.5	**1_I** (tubular)	54
40	GETMAV	3.76	12.7	**1_I** (tubular)	54
Two-dimensional aggregate					
41	LUFTOW	3.60	9.9	**2_I** (flat)	55
Sb(III) structures					
Zero-dimensional aggregates					
42	WEWDOT	3.67	10.6	**0_I**	56
43	YUGSOK	3.78	17.3	**0_I**	57
44	TOMQAP	3.85	15.1	**0_I**	58
45	MOZPAU	3.95	14.3	**0_I**	59
One-dimensional aggregates					
46	SEKGEW	3.37	0.2	**1_I** (linear)	60
47	SEKGIA	3.38	2.4	**1_I** (linear)	60
48	HIJRID	3.61	5.4	**1_I** (helical)	61
49	HORPIP	3.94	17.5	**1_I** (helical)	62
Bi(III) structures					

Zero-dimensional aggregates					
50	BIQVAA	3.51	4.5	**0_I**	63
51	VICKAV	3.52	3.7	**0_I**	64
52	BIQGEP	3.55	5.9	**0_I**	63
53	WOXFUM	3.59	14.1	**0_I**	64
54	WAZWOL	3.67	4.9	**0_I**	65
55	LONJUV	3.71	11.0	**0_I**	66
56	MATQEF	3.74	13.7	**0_I**	67
57	HIJROJ	3.76	13.1	**0_I**	68
58	IZUHIV	3.76	13.4	**0_I**	69
59	WAZWUR	3.78	3.9	**0_I**	65
60	NOCGES01	3.92	18.2	**0_I**	69
61	DUGLIC	3.72	13.2	**0_I**	70
62	BITRPH11	3.79	12.7	**0_I**	71
		3.94	13.0		
One-dimensional aggregates					
63	HAQMAP	3.37	2.0	**1_I** (linear)	72
64	XAJHUO	3.55	13.0	**1_I** (linear)	73
		3.59	13.8		
		3.56	12.4		
		3.61	14.2		
65	LEYZIA	3.93	15.2	**1_I** (linear)	56
66	ETUXIB	3.85	12.3	**1_I** (zigzag)	74
67	KIKRED	3.42	9.8	**1_I** (helical)	75
		3.71	13.0		

68	PAFQIY	3.73	2.8	**1_I** (helical)	76
69	MSTLBI02	3.93	15.1	**1_I** (helical)	77
70	DUGKOH	3.28	1.8	**1_IV** (stepped)	78
		3.40	2.1		
71	DUGKIB	3.27	4.9	**1_IV** (stepped)	78
		3.36	3.7		

Table 4 Geometric parameters characterising Se(lp)…π(arene) interactions in **72**–**124**

Compound	CSD ref. code	*d* (Å)	θ (º)	Motif	Ref.
Se(II) structures					
Zero-dimensional aggregates					
72	NARWUA	3.47	5.0	**0_I**	80
73	ERUWIY	3.49	8.6	**0_I**	81
74	WARJIK	3.49	12.2	**0_I**	82
75	OXAWOA	3.51	10.3	**0_I**	83
76	QOMTIX	3.57	14.2	**0_I**	84
77	WUSJUR	3.57	16.4	**0_I**	85
78	SAGTOM	3.58	11.2	**0_I**	86
79	SADVOK	3.66	11.2	**0_I**	87
80	EVAVED	3.67	8.2	**0_I**	88
81	ISUJAI	3.69	19.0	**0_I**	89
82	AXAGOW	3.70	12.3	**0_I**	90
83	MIVYUN	3.86	13.3	**0_I**	91
84	QOJWET	3.87	18.9	**0_I**	92
85	QODXUE	3.53	16.7	**0_I**	93
86	ZOSSIL	3.84	12.8	**0_I**	94
87	FUXTOI	3.91	11.2	**0_II**	95
88	RIHVEL	3.75	18.3	**0_III**	96
		3.92	19.4		
89	CENBAA	3.36	8.0	**0_IV**	97
		3.45	4.7		

90	BEYCIT	3.71	14.9	**0_I**	98
91	BEYCUF	3.50	9.0	**0_I**	98
92	JOLZER	3.48	1.6	**0_I**	99
93	JANKIT	3.59	12.4	**0_I**	100
94	WUSKAY	3.43	10.6	**0_V**	85
		3.91	16.8		
One-dimensional aggregates					
95	UJIVUF	3.60	12.8	**1_I** (linear)	101
96	ERUVUJ	3.63	8.5	**1_I** (linear)	81
97	TOVQEC	3.64	14.8	**1_I** (linear)	102
98	WARLAE	3.78	7.8	**1_I** (linear)	82
99	ZOMMIZ	3.83	6.8	**1_I** (linear)	103
100	OPUYII	3.84	15.4	**1_I** (linear)	104
101	ZOMMOF	3.85	16.1	**1_I** (linear)	103
102	SENGOH01	3.91	12.6	**1_I** (linear)	105
103	XEYZIM	3.95	9.9	**1_I** (linear)	106
104	ZUBWAW	3.48	4.5	**1_I** (zigzag)	107
105	QOVGAL	3.58	18.0	**1_I** (zigzag)	108
106	EDIGUU02	3.75	4.2	**1_I** (zigzag)	105
107	XAYCIL	3.91	19.3	**1_I** (zigzag)	109
108	XAYCUX	3.97	19.8	**1_I** (zigzag)	109
109	GIYJUV	3.98	9.5	**1_I** (zigzag)	110
110	DIZSIQ	3.48	8.6	**1_I** (helical)	111
111	AFUPEY	3.51	16.4	**1_I** (helical)	112
112	GAQQEW	3.54	17.3	**1_I** (helical)	113

113	LEDZIF	3.57	11.8	**1_I** (helical)	114
114	ZOGFIM	3.74	17.2	**1_I** (helical)	115
115	WEKWOA	3.53	15.3	**1_I** (linear)	116
116	HOGBOW	3.69	8.4	**1_I** (linear)	117
117	COFBAC	3.87	9.4	**1_I** (linear)	118
118	LIFFUD	3.95	18.8	**1_I** (linear)	119
119	ICEWIY	3.52	11.6	**1_I** (zigzag)	120
120	WARKOR	3.54	15.2	**1_II** (linear)	121
		3.79	6.7		
121	IGIXIH	3.69	17.0	**1_II** (linear)	82
122	REDGUE	3.94	16.8	**1_V** (twisted)	122
123	SUWFIB	3.68	2.8	**1_I** (linear)	123
Se(IV) structure					
One-dimensional aggregate					
124	PAHFOV	3.56	2.4	**1_I** (zigzag)	124

Table 5 Geometric parameters characterising Te(lp)…π(arene) interactions in **125**–**157**

Compound	CSD ref. code	*d* (Å)	θ (º)	Motif	Ref.
Te(II) structures					
Zero-dimensional aggregates					
125	**POYGIT01**	3.61	8.8	**0_I**	125
126	**HUJROV**	3.67	14.3	**0_I**	126
127	**VUBPIT**	3.69	8.9	**0_I**	127
		3.72	12.1		
128	**TOWZOW**	3.54	5.7	**0_I**	128
129	**TOWYEL**	3.58	9.8	**0_I**	128
130	**TOXCAM**	3.62	14.1	**0_I**	128
131	**KIBTEW**	3.63	14.4	**0_I**	129
132	**TOXBIT**	3.65	9.3	**0_I**	128
133	**TOXBOZ**	3.68	12.7	**0_I**	128
134	**TOXCIU**	3.69	10.4	**0_I**	128
135	**TOXCOA**	3.71	9.9	**0_I**	128
136	**TOWYIP**	3.72	9.9	**0_I**	128
137	**TOWZAI**	3.78	16.6	**0_I**	128
138	**BETDAG01**	3.85	18.6	**0_I**	130
One-dimensional aggregates					
139	**NECVOI**	3.48	12.7	**1_I** (linear)	131
140	**HUHMII**	3.67	10.0	**1_I** (linear)	126
		3.58	1.5		
141	**WARLEI**	3.74	5.3	**1_I** (linear)	82

142	**WARJOQ**	3.85	3.7	**1_I** (linear)	82
143	**WARKEH**	3.92	4.2	**1_I** (linear)	82
		3.92	4.8		
144	**HUJRAH**	3.93	8.1	**1_I** (linear)	126
145	**UJOSES**	3.62	7.5	**1_I** (zigzag)	132
146	**GUFPAA**	3.79	11.6	**1_I** (zigzag)	133
147	**EHUSOQ**	3.62	0.8	**1_I** (helical)	134
148	**GUDGET**	3.71	11.1	**1_I** (helical)	135
149	**YUXQEO**	3.55	9.3	**1_I** (linear)	136
150	**MUWFIU**	3.72	8.5	**1_I** (zigzag)	137
151	**INIXAF**	3.62	9.3	**1_I** (linear)	138
Te(IV) structures					
152	**RATFID**	3.51	11.7	**0_I**	139
153	**IRUKEM**	3.58	9.9	**0_I**	140
154	**UJOSIW**	3.64	8.1	**1_I** (zigzag)	132
155	**KAKCOP**	3.76	19.4	**1_I** (zigzag)	141
156	**WARNEK**	3.83	18.0	**1_I** (zigzag)	82
157	**HAQHOY**	3.85	9.6	**1_I** (zigzag)	142

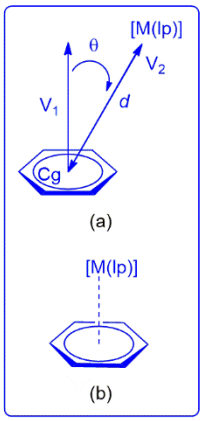

Fig. 1 Search protocols for element(lp)···π(arene) interactions: (a) geometric restrictions where *d* (Å) is the distance between the ring centroid, Cg, and the element under consideration, and θ (º) is the angle between the normal to the arene ring, V_1, and the vector, V_2, between the ring centroid and the element, and (b) representation of a delocalised element(lp)···π(arene) interaction where the lone-pair interacts equally with all carbon atoms of the arene ring.

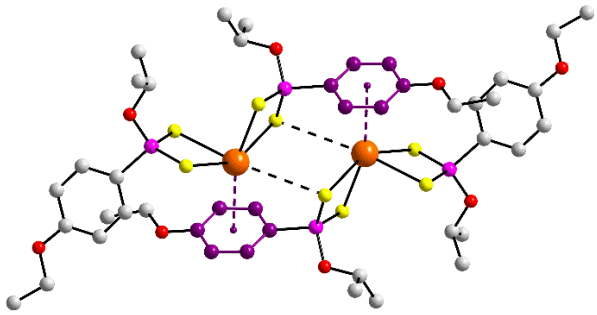

Fig. 2 Supramolecular association in the structure of $\{Pb[S_2P(O\text{-}iPr)(OC_6H_4OEt\text{-}4)]_2\}_2$ with Pb(lp) ···π(arene) and Pb···S secondary interactions shown as purple and black dashed lines, respectively. Colour code in this and subsequent diagrams: orange, element donating the lone-pair of electrons; yellow, sulphur; pink, phosphorus; red, oxygen; grey, carbon. The arene ring participating in the element(lp)···π(arene) interaction is highlighted in purple. All but acidic hydrogen atoms (green) are omitted.

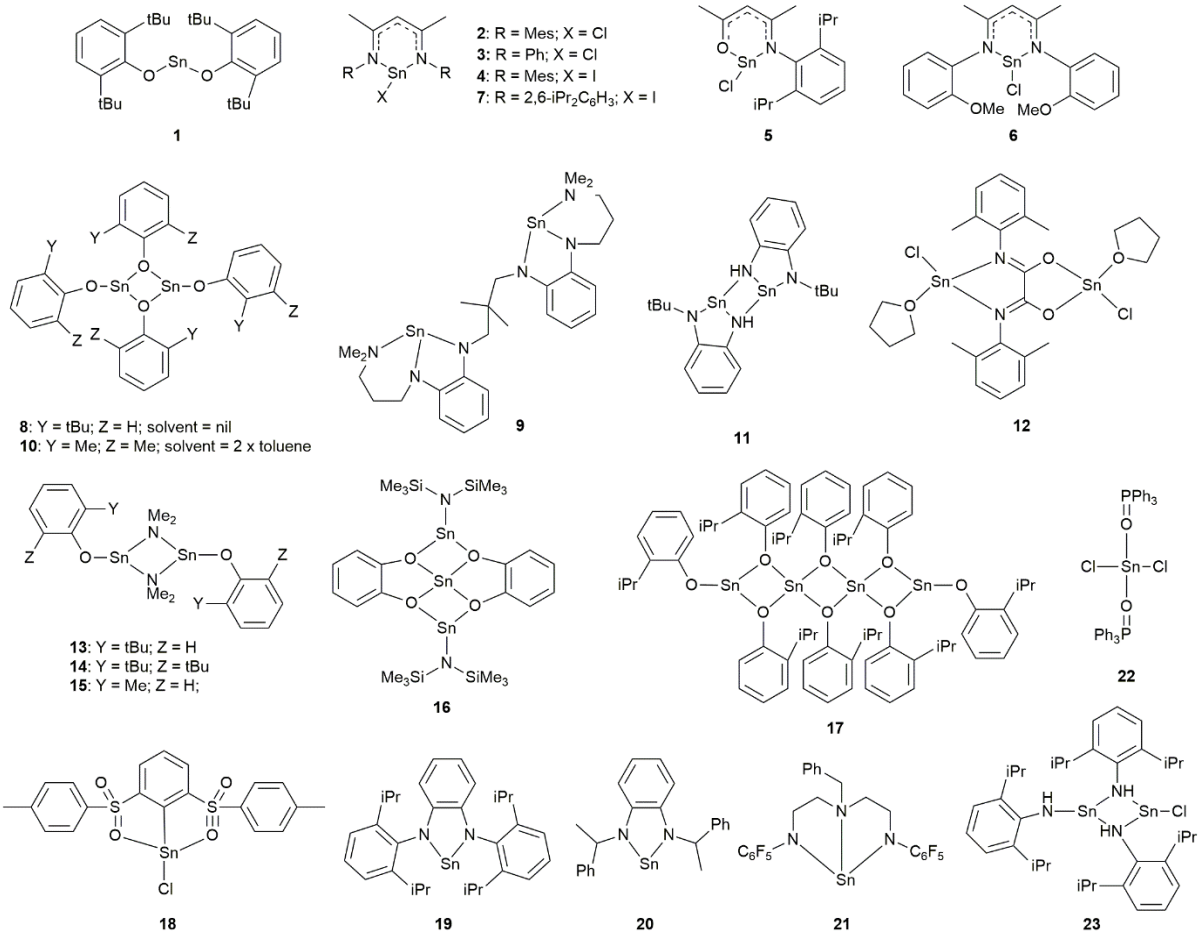

Fig. 3 Chemical structure diagrams for tin(II) compounds **1**–**23** which form Sn(lp)···π(arene) interactions leading to zero- (**1**–**17**) and one- (**18**–**23**) dimensional aggregation patterns.

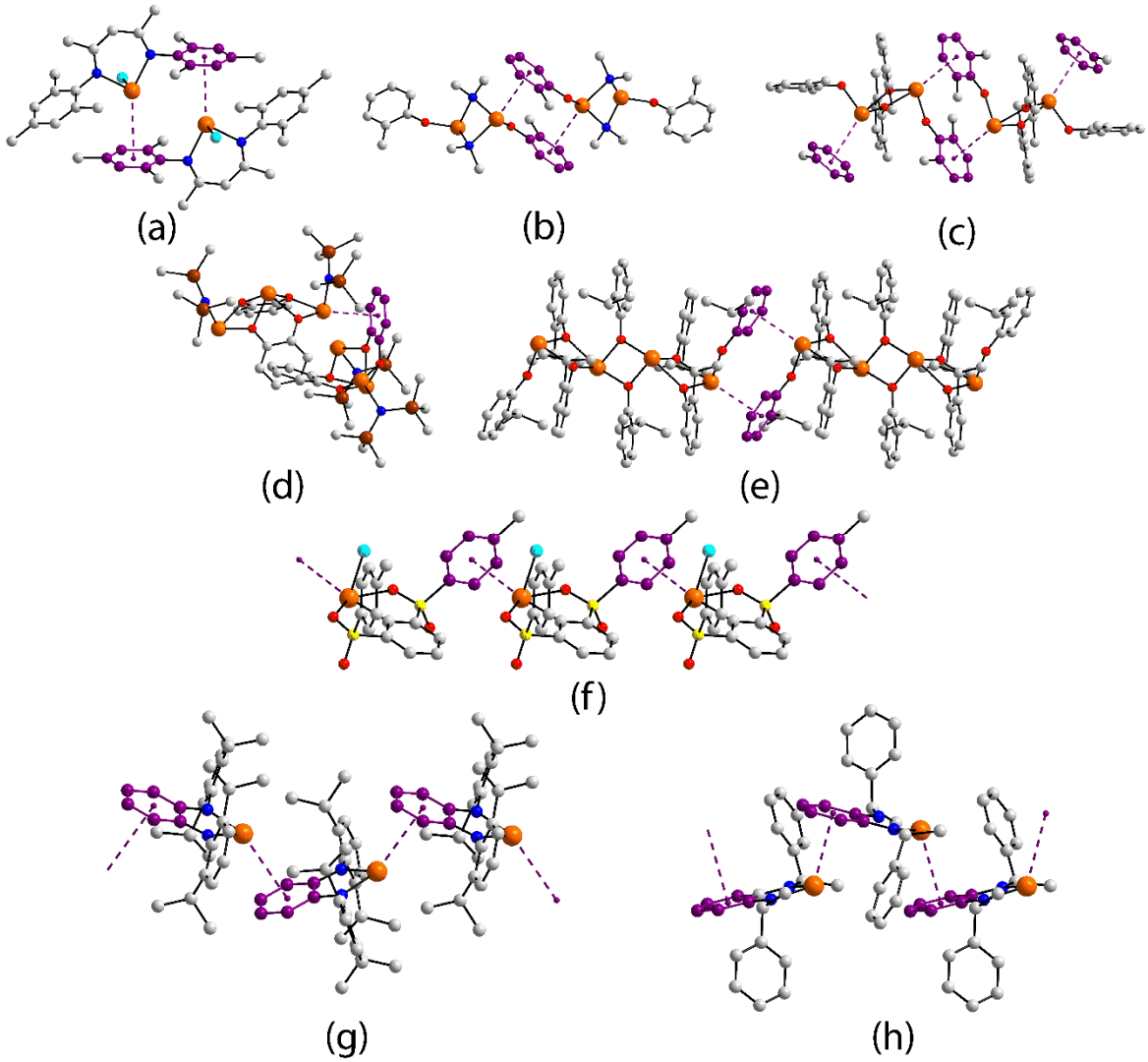

Fig. 4 Supramolecular aggregates sustained by Sn(lp)···π(arene) interactions in the crystal structures of (a) **2**, (b) **15**, (c) **10**, (d) **16**, (e) **17**, (f) **18**, (g) **19** and (h) **20**. Additional colour code: blue, nitrogen; brown, silicon.

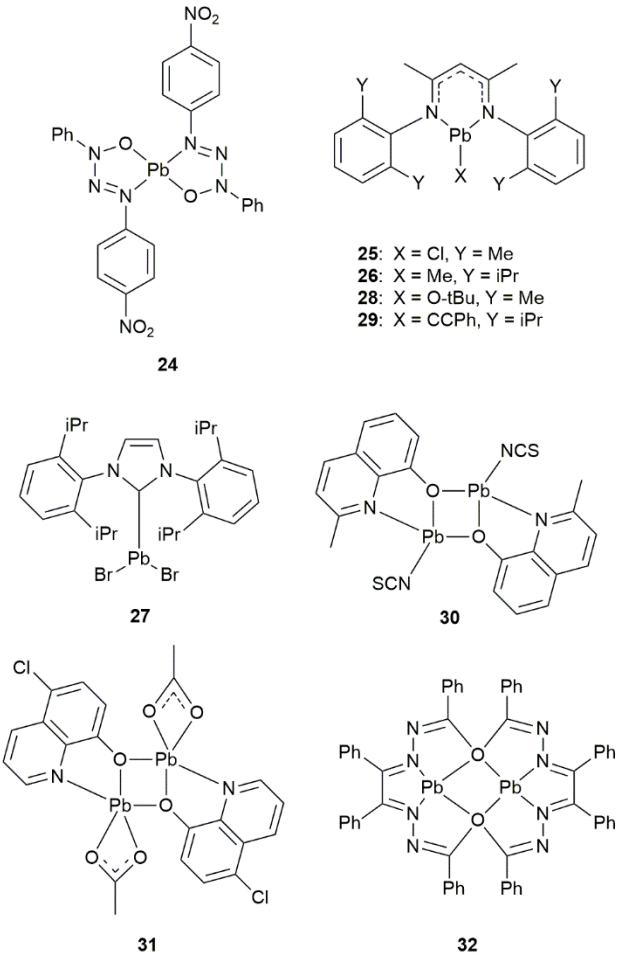

Fig. 5 Chemical structure diagrams for lead(II) compounds **24**–**32** which form Pb(lp)···π(arene) interactions leading to zero- (**24**–**28**) and one- (**29**–**32**) dimensional aggregation patterns.

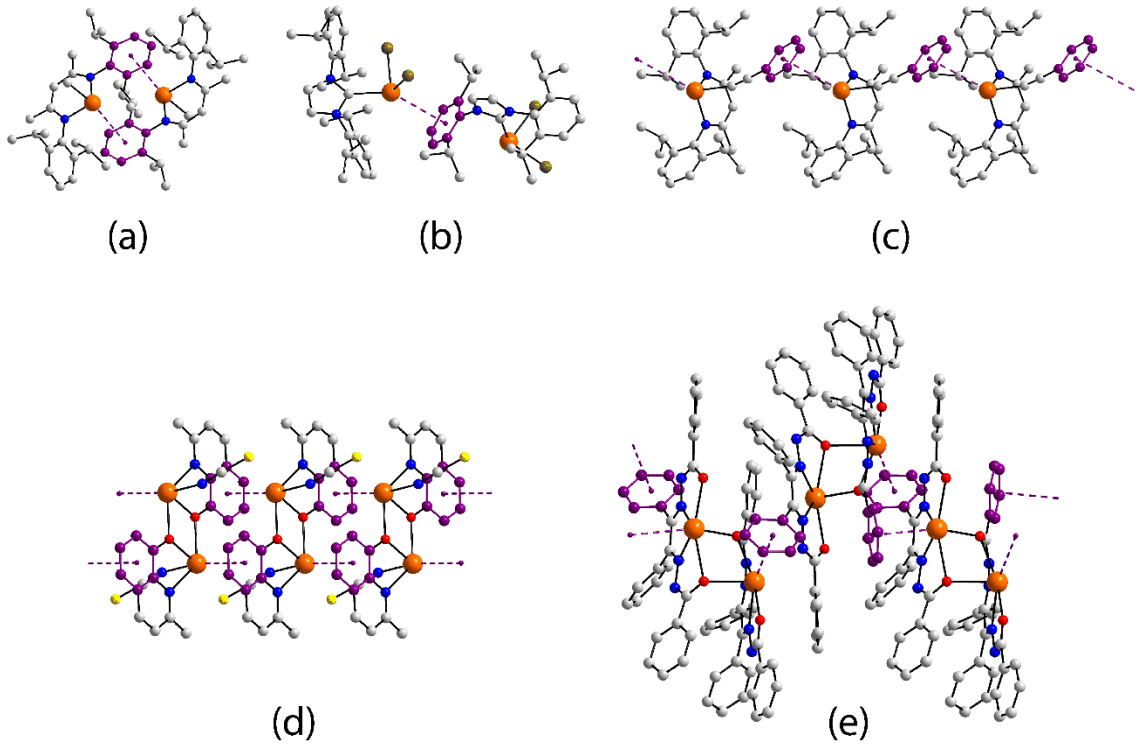

Fig. 6 Supramolecular aggregates sustained by Pb(lp)···π(arene) interactions in the crystal structures of (a) **26**, (b) **27**, (c) **29**, (d) **30** and (e) **32**. Additional colour code: olive-green, bromide.

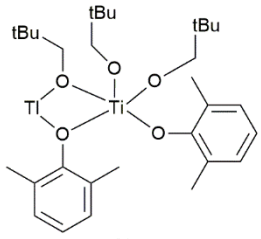

33

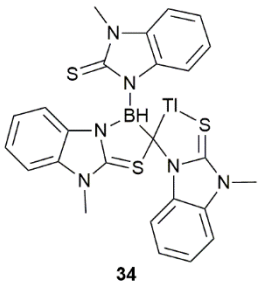

34

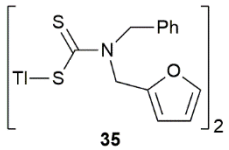

35

Fig. 7 Chemical structure diagrams for thallium(II) compounds **33**–**35** which form Tl(lp)···π(arene) interactions leading to zero- (**33** and **34**) and two- (**35**) dimensional aggregation patterns.

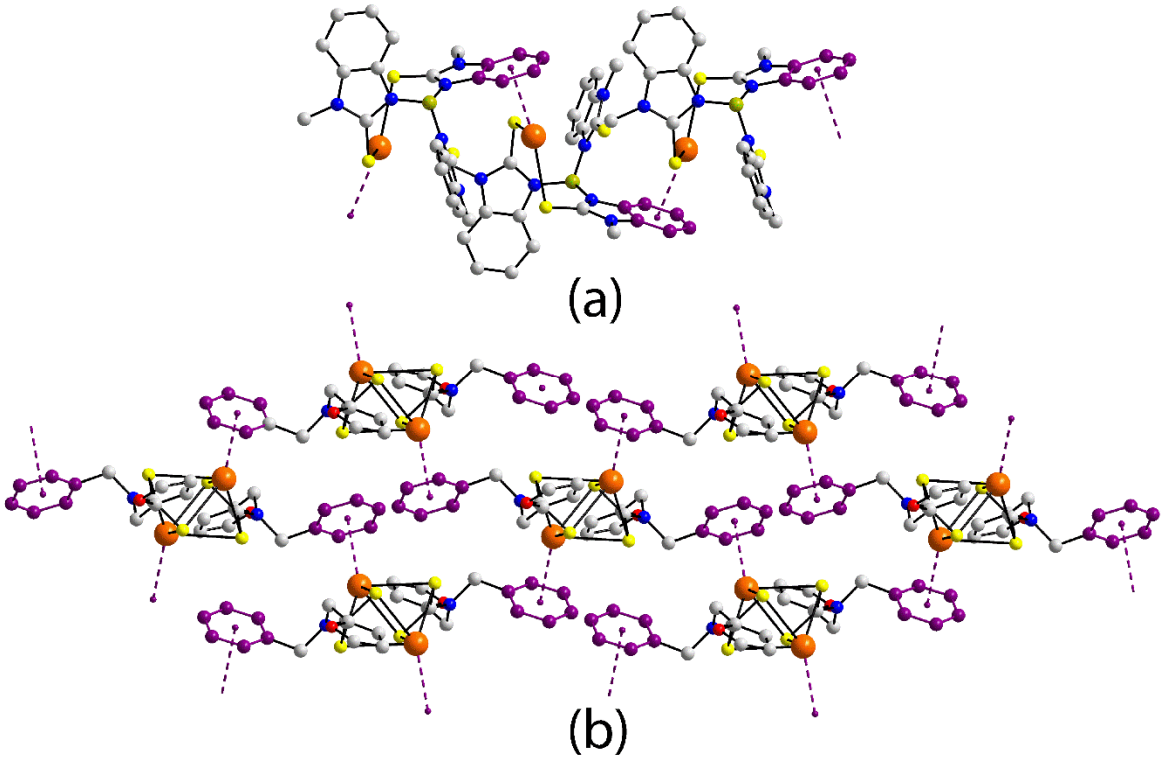

Fig. 8 Supramolecular aggregates sustained by Tl(lp)···π(arene) interactions in the crystal structures of (a) **34** and (b) **35**. Additional colour code: lime, boron.

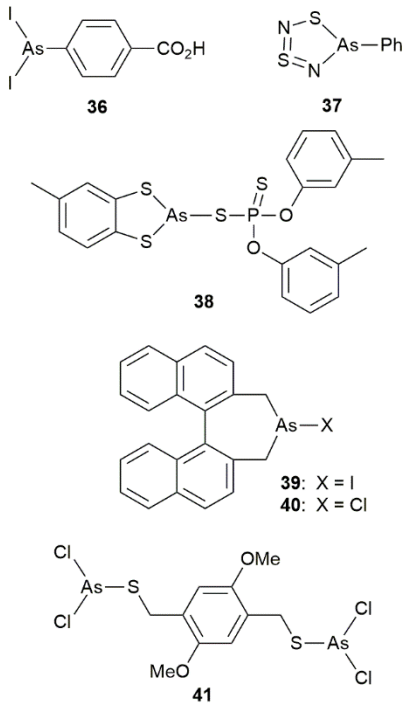

Fig. 9 Chemical structure diagrams for arsenic(III) compounds **36**–**41** which form As(lp)···π(arene) interactions leading to zero- (**36**–**40**) and two- (**41**) dimensional aggregation patterns.

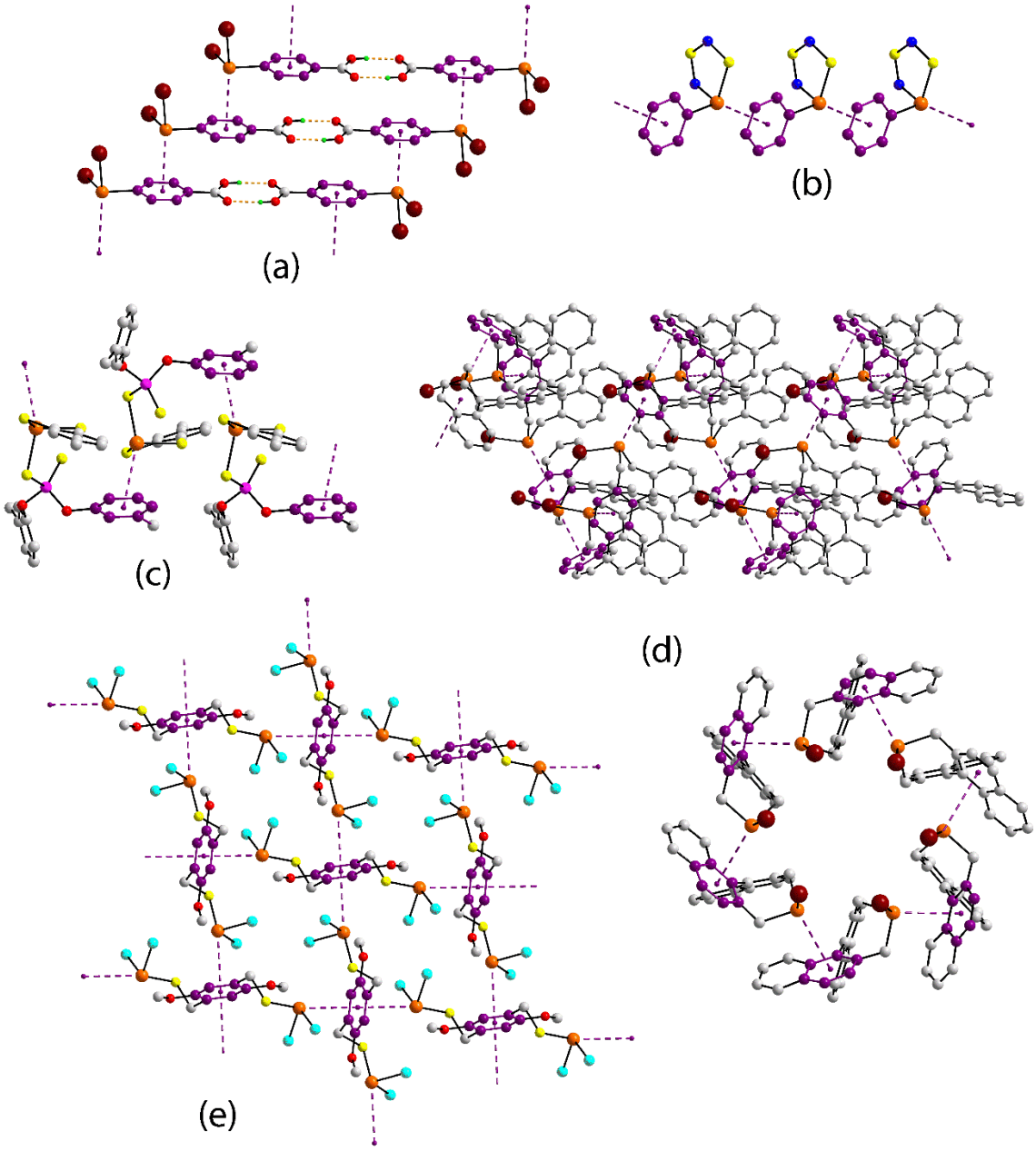

Fig. 10 Supramolecular aggregates sustained by As(lp)···π(arene) interactions in the crystal structures of (a) **36**, (b) **37**, (c) **38**, (d) **39** and (e) **41**. Additional colour code: dark-red, iodide.

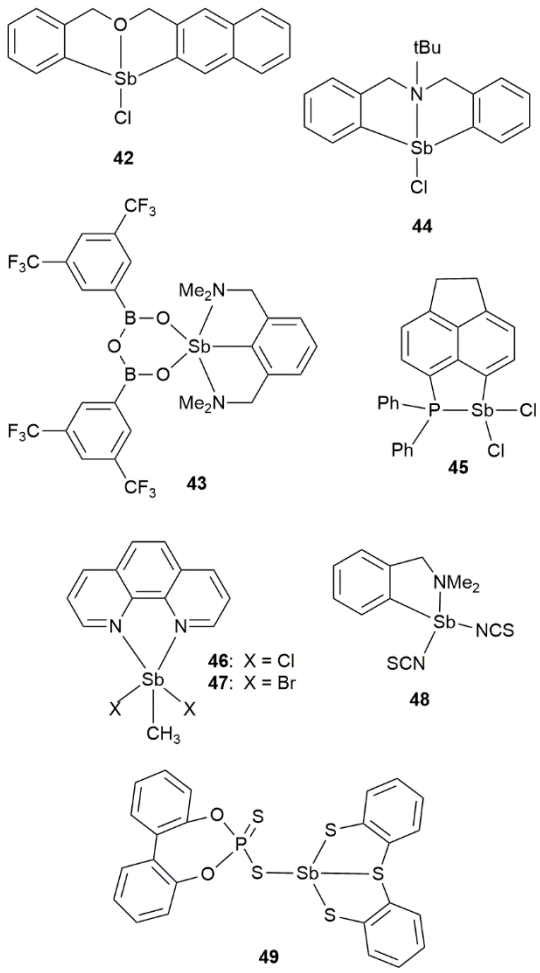

Fig. 11 Chemical structure diagrams for antimony(III) compounds **42**–**49** which form Sb(lp)···π(arene) interactions leading to zero- (**42**–**45**) and one- (**46**–**49**) dimensional aggregation patterns.

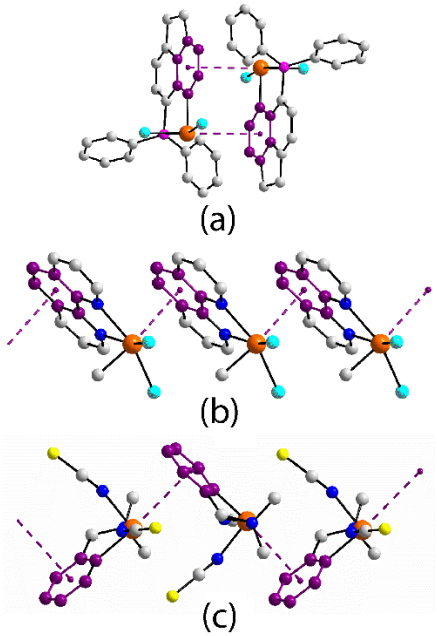

Fig. 12 Supramolecular aggregates sustained by Sb(lp)···π(arene) interactions in the crystal structures of (a) **45**, (b) **46** and (c) **48**.

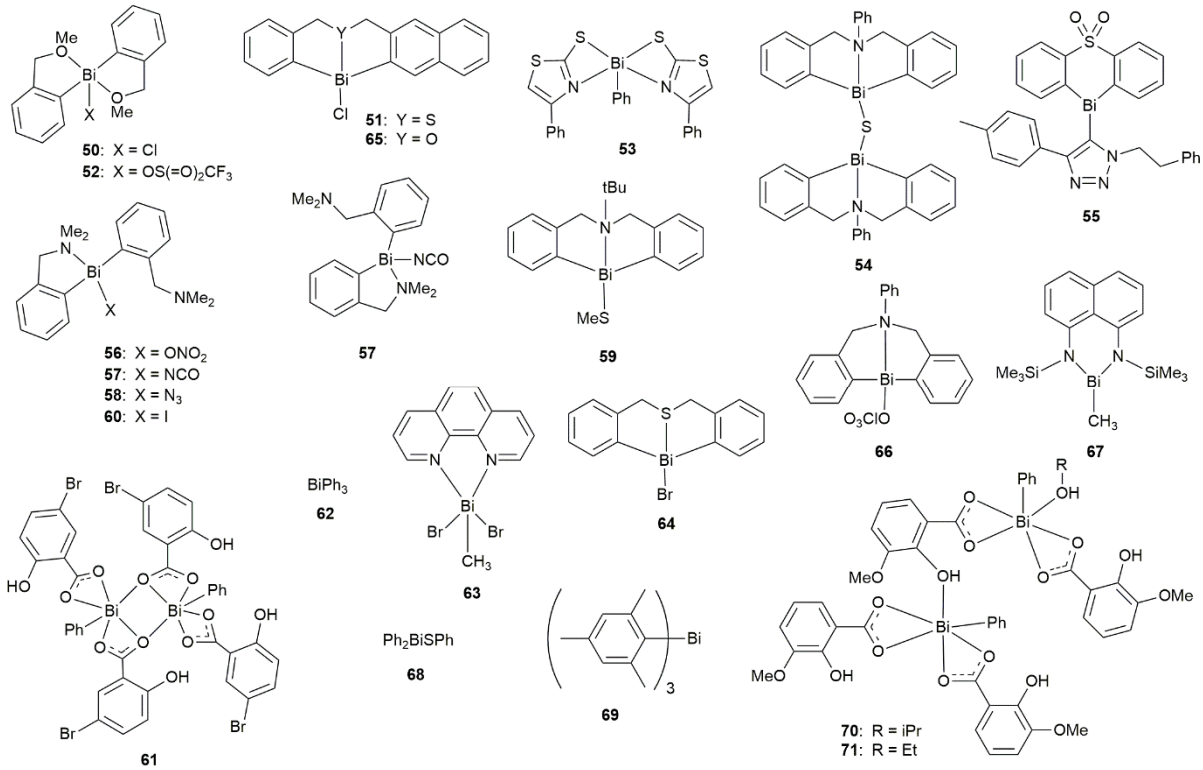

Fig. 13 Chemical structure diagrams for bismuth(III) compounds **50**–**71** which form Bi(lp)···π(arene) interactions leading to zero- (**50**–**62**) and one- (**63**–**71**) dimensional aggregation patterns.

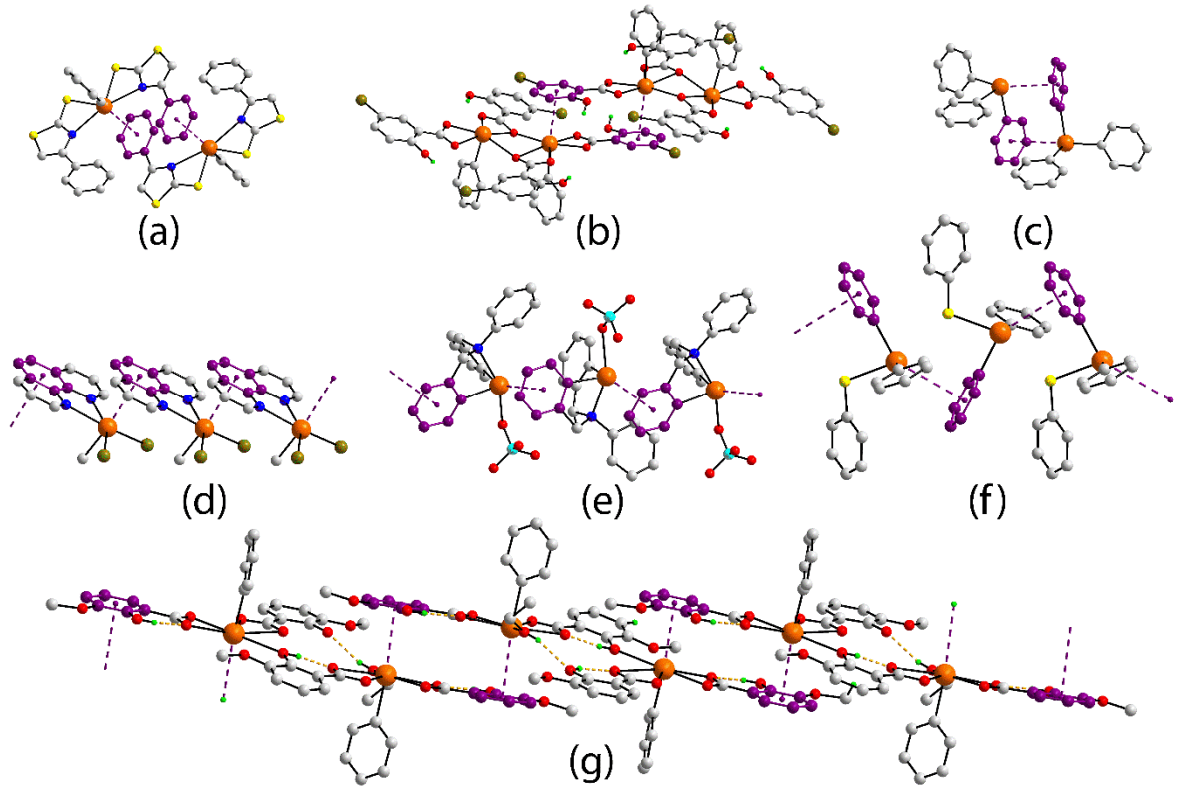

Fig. 14 Supramolecular aggregates sustained by Bi(lp)···π(arene) interactions in the crystal structures of (a) **53**, (b) **61**, (c) **62**, (d) **63**, (e) **66**, (f) **68** and (g) **71**. Additional colour code: cyan, chloride; green, hydrogen.

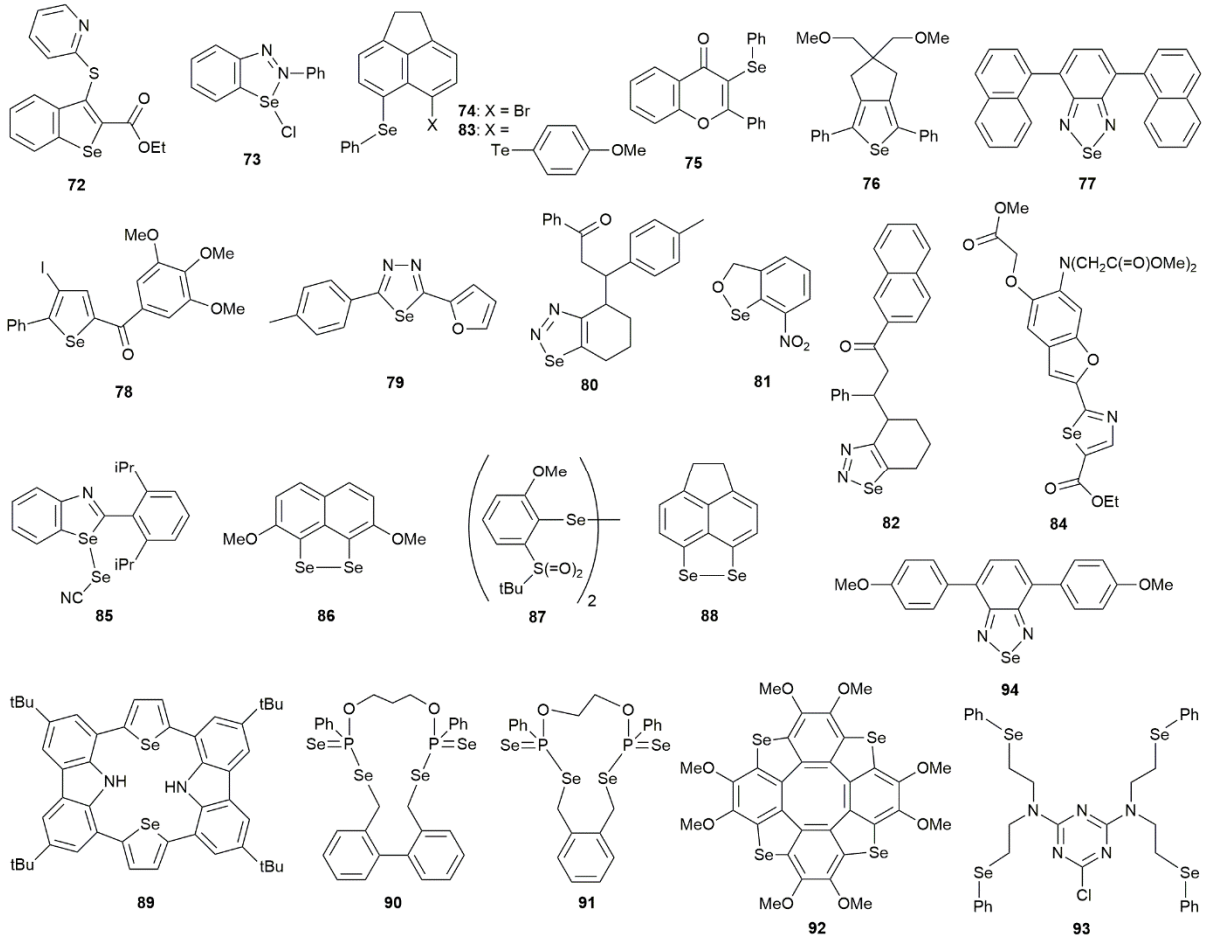

Fig. 15 Chemical structure diagrams for selenium(II) compounds **72–94** which form Se(lp)···π(arene) interactions leading to zero-dimensional aggregation patterns.

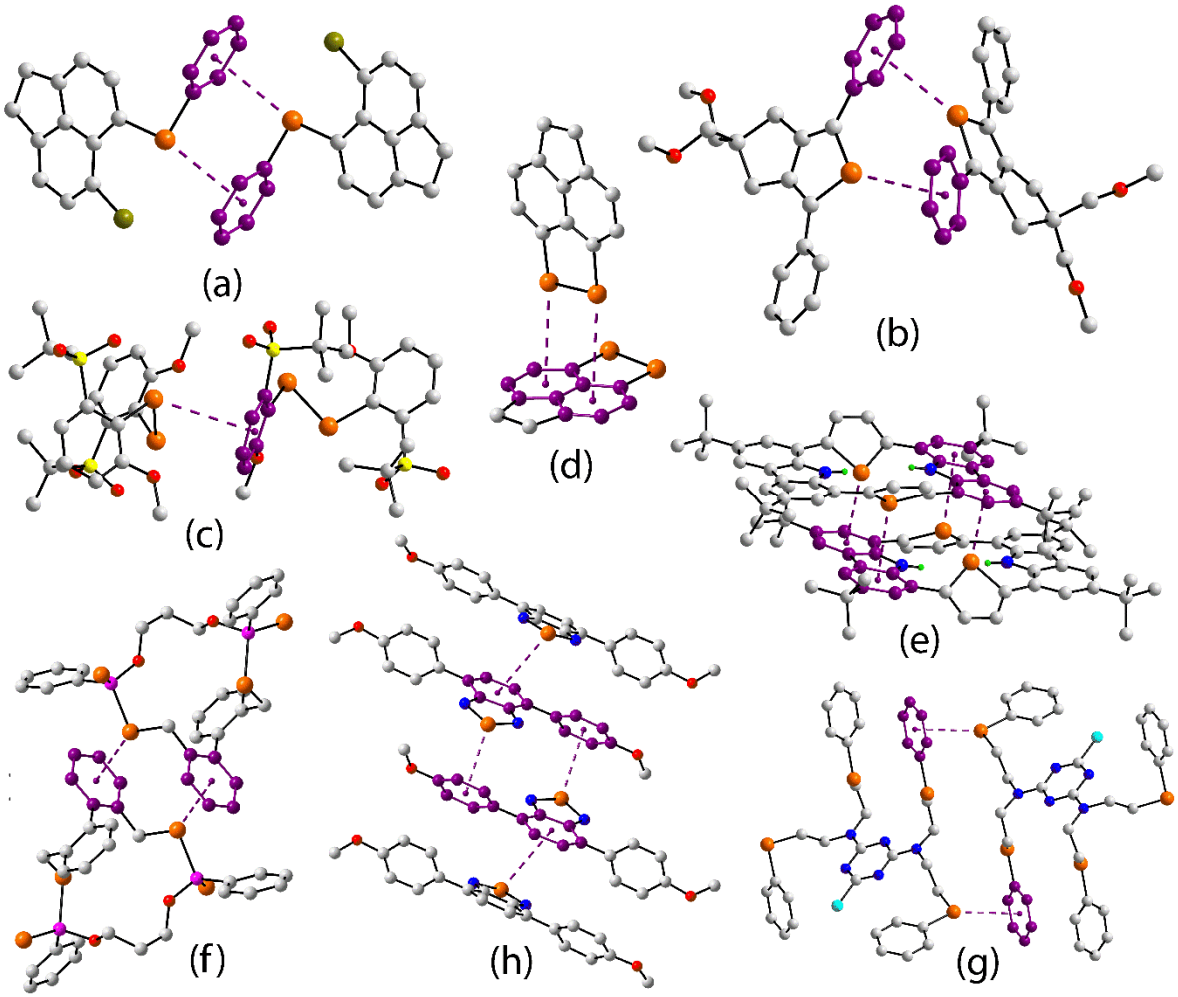

Fig. 16 Zero-dimensional, supramolecular aggregates sustained by Se(lp)···π(arene) interactions in the crystal structures of (a) **74**, (b) **76**, (c) **87**, (d) **88**, (e) **89**, (f) **90**, (g) **93** and (h) **94**.

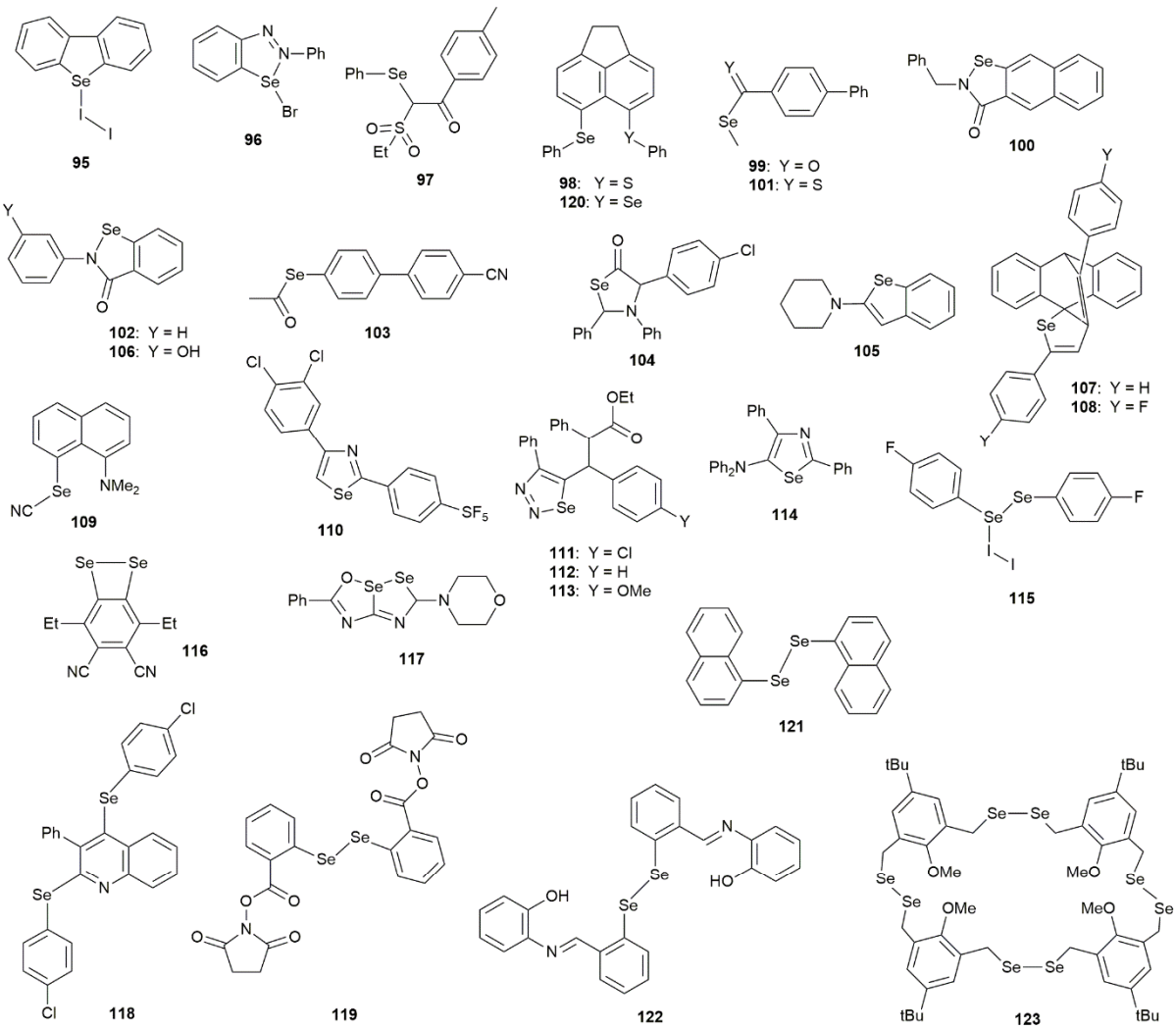

Fig. 17 Chemical structure diagrams for selenium(II) compounds **95–123** which form Se(lp)···π(arene) interactions leading to one-dimensional aggregation patterns.

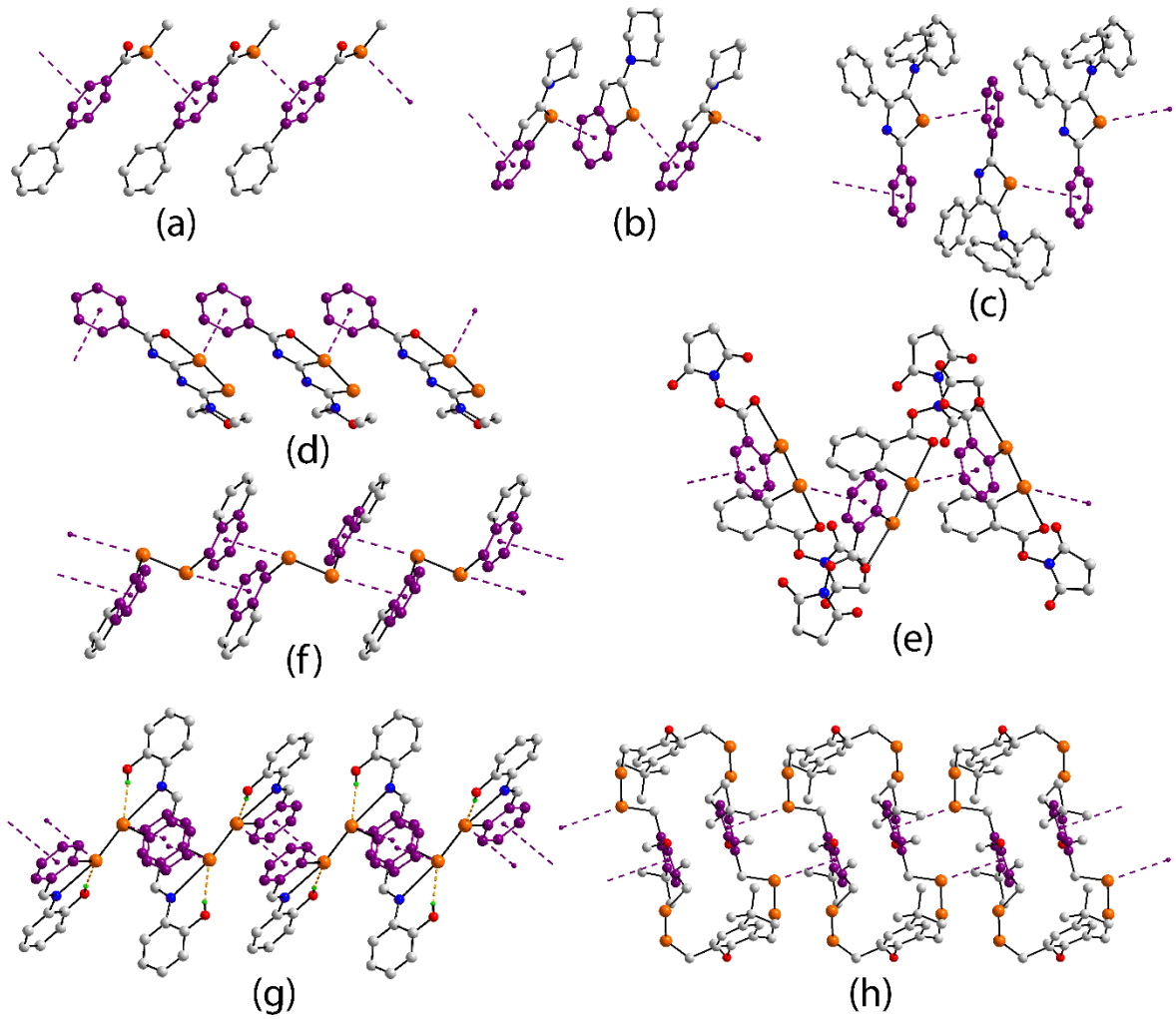

Fig. 18 One-dimensional, supramolecular aggregates sustained by Se(lp)···π(arene) interactions in the crystal structures of (a) **99**, (b) **105**, (c) **114**, (d) **117**, (e) **119**, (f) **121**, (g) **122** and (h) **123**.

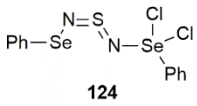

124

Fig. 19 Chemical structure diagram for selenium(IV) compound **124** which forms Se(lp)···π(arene) interactions leading to a one-dimensional aggregate.

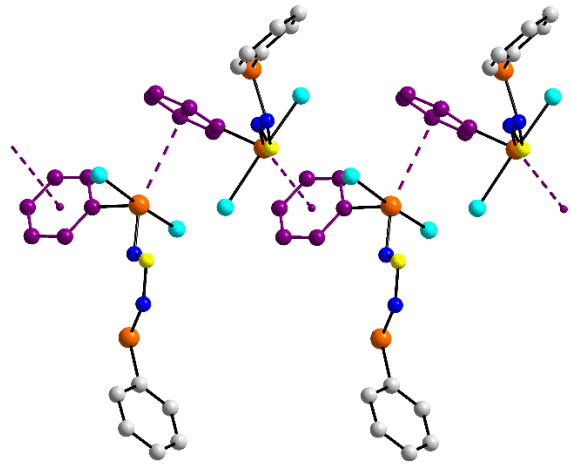

Fig. 20 One-dimensional, supramolecular aggregate sustained by Se(lp)···π(arene) interactions in the crystal structure of **124**.

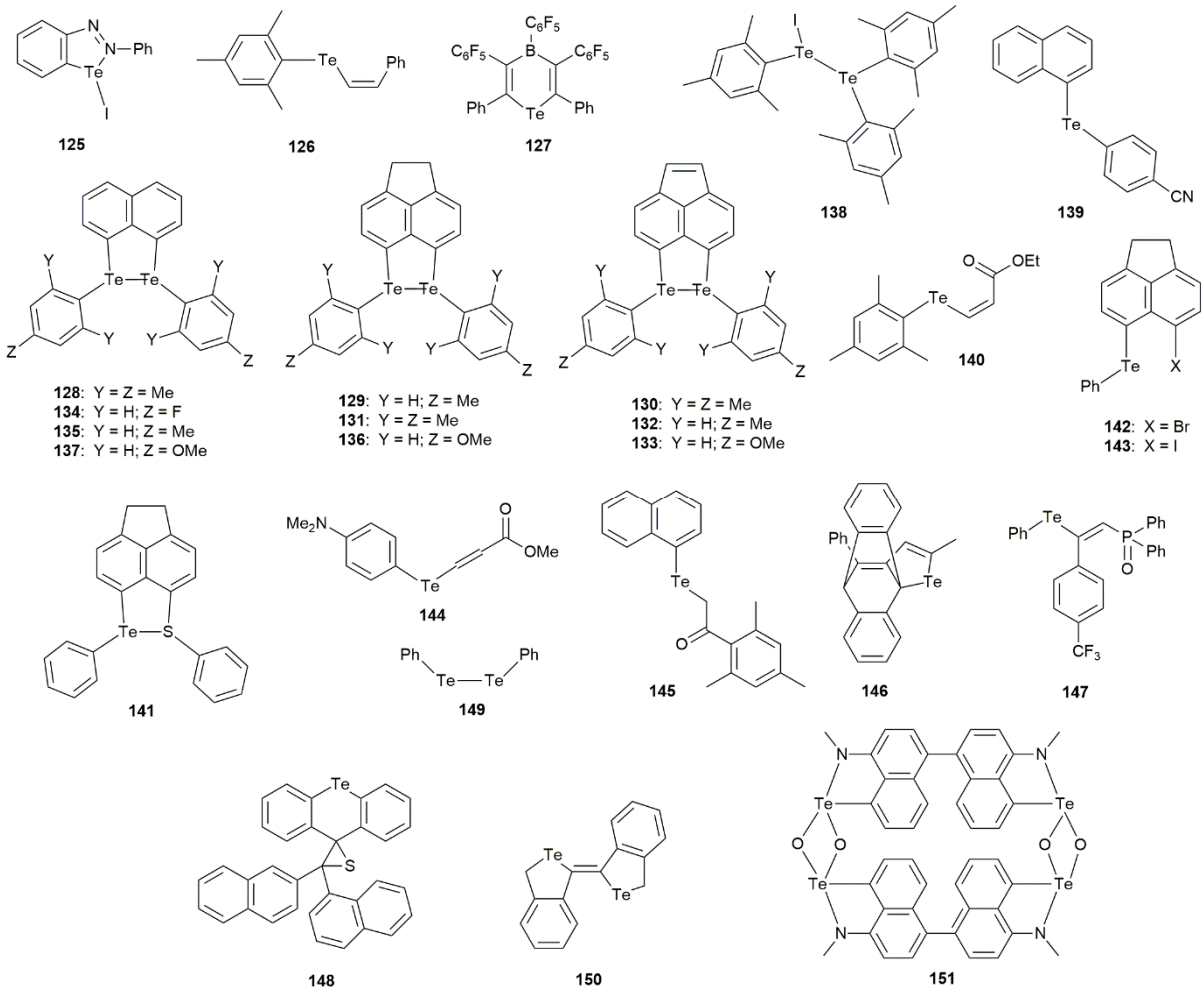

Fig. 21 Chemical structure diagrams for tellurium(II) compounds **125**–**151** which form Te(lp)···π(arene) interactions leading to zero- (**125**–**138**) and one- (**139**–**151**) dimensional aggregation patterns.

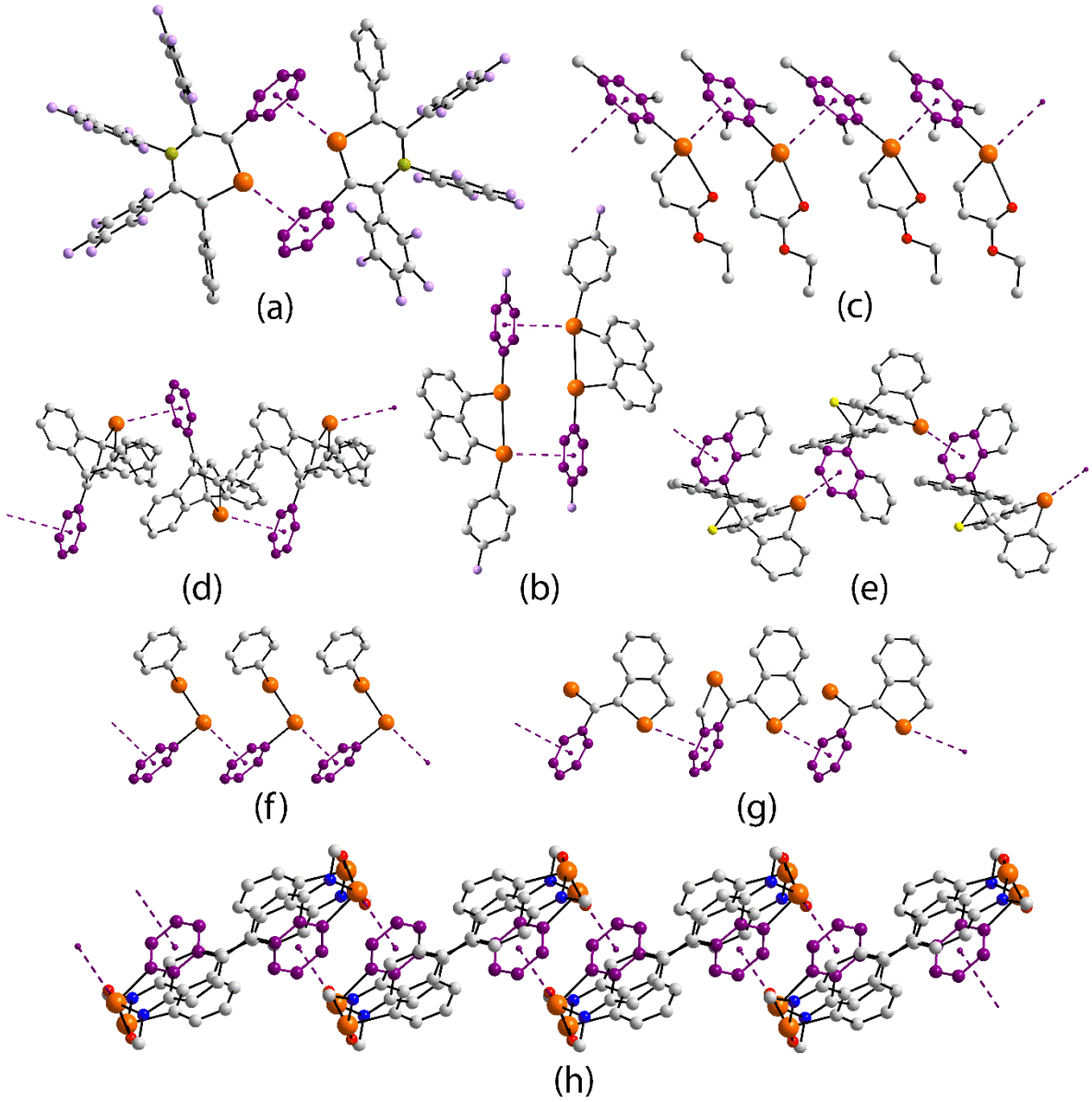

Fig. 22 Supramolecular aggregates sustained by Te(lp)···π(arene) interactions in the crystal structures of (a) **127**, (b) **134**, (c) **140**, (d) **146**, (e) **148**, (f) **149**, (g) **150** and (h) **151**. Additional colour code: mauve, fluoride.

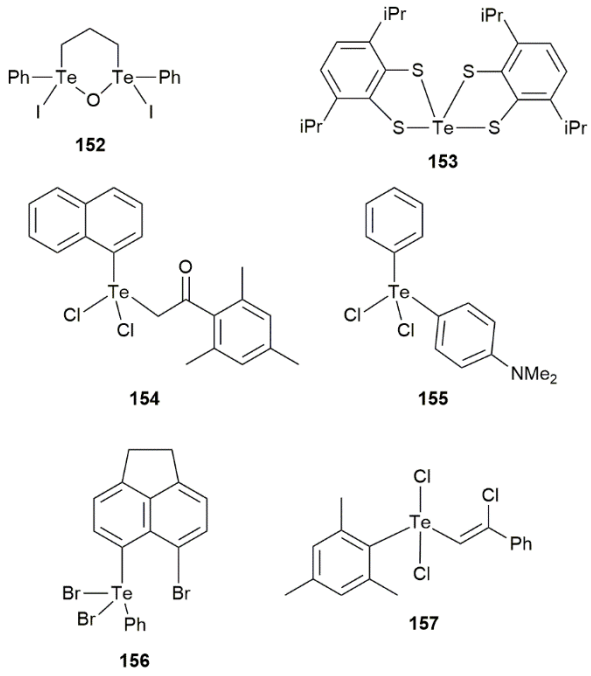

Fig. 23 Chemical structure diagrams for tellurium(IV) compounds **152**–**157** which form Te(lp)···π(arene) interactions leading to zero- (**152** and **153**) and one- (**154**–**157**) dimensional aggregation patterns.

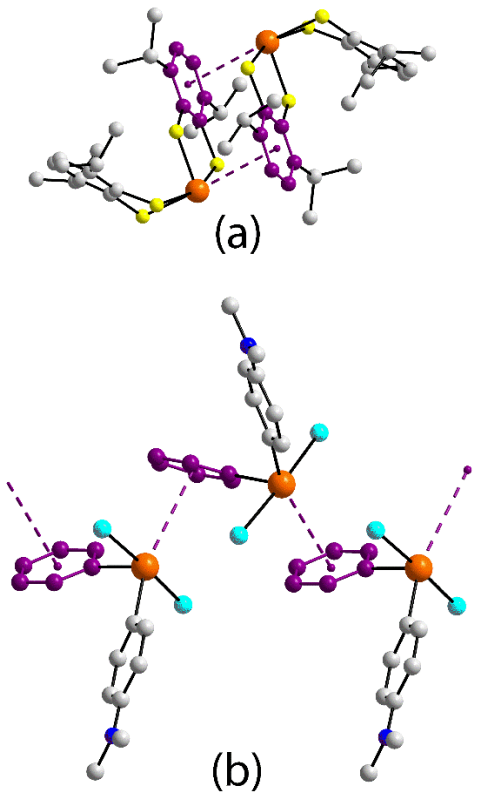

Fig. 24 Supramolecular aggregates sustained by Te(lp)···π(arene) interactions in the crystal structures of (a) **153** and (b) **155**.

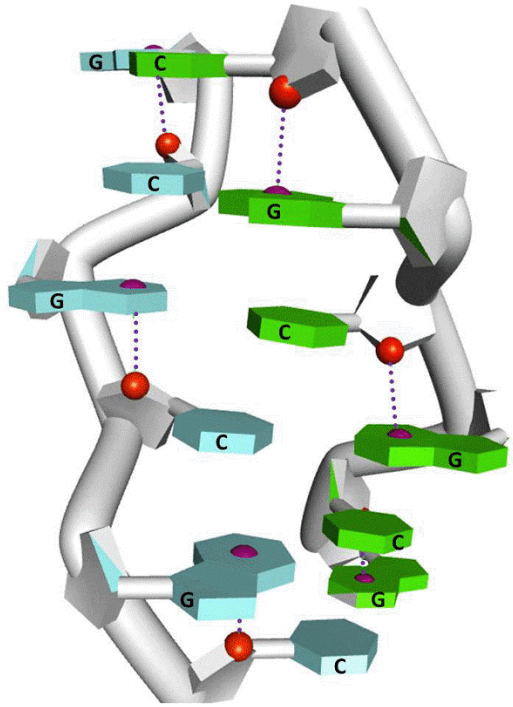

Fig. 25 Illustration of cytidine-sugar-O atom···π(pyrimidine) interaction, thought to stabilise the conformation found in the left-handed Z-DNA duplex.

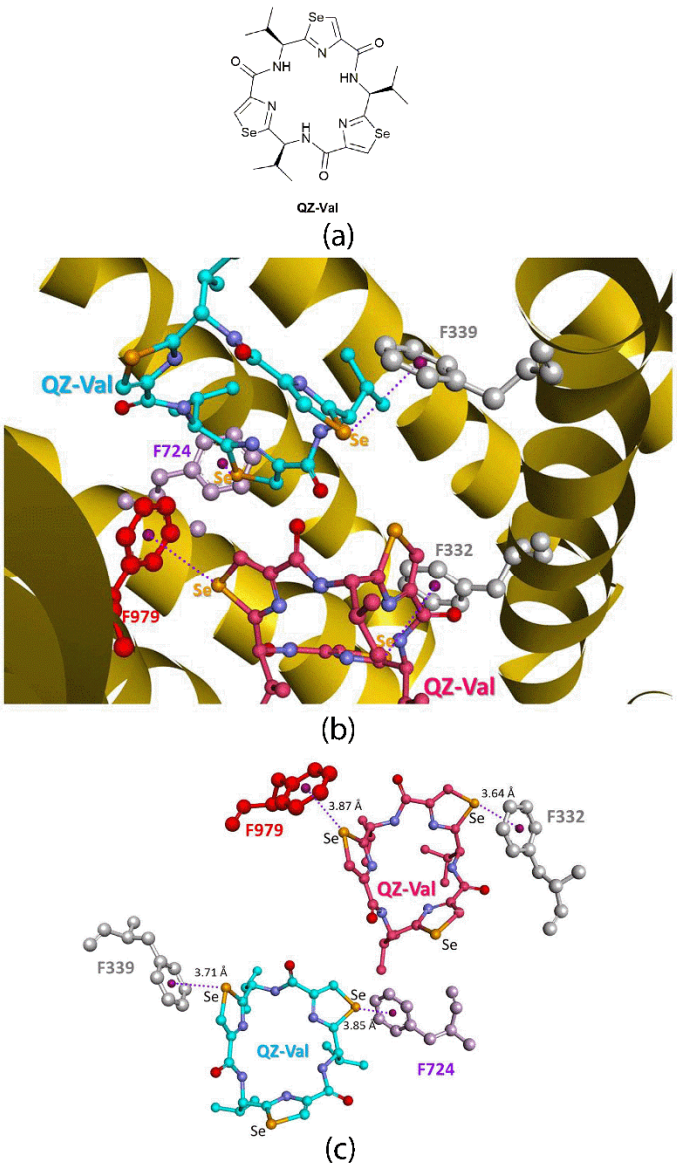

Fig. 26 (a) Chemical diagram of the cyclic hexapeptide inhibitor QZ-Val, (b) view of the interaction between P-glycoprotein and QZ-Val *via* selenium(lp)···π(arene) interactions and (c) detail of the selenium(lp)···π(arene) interactions.

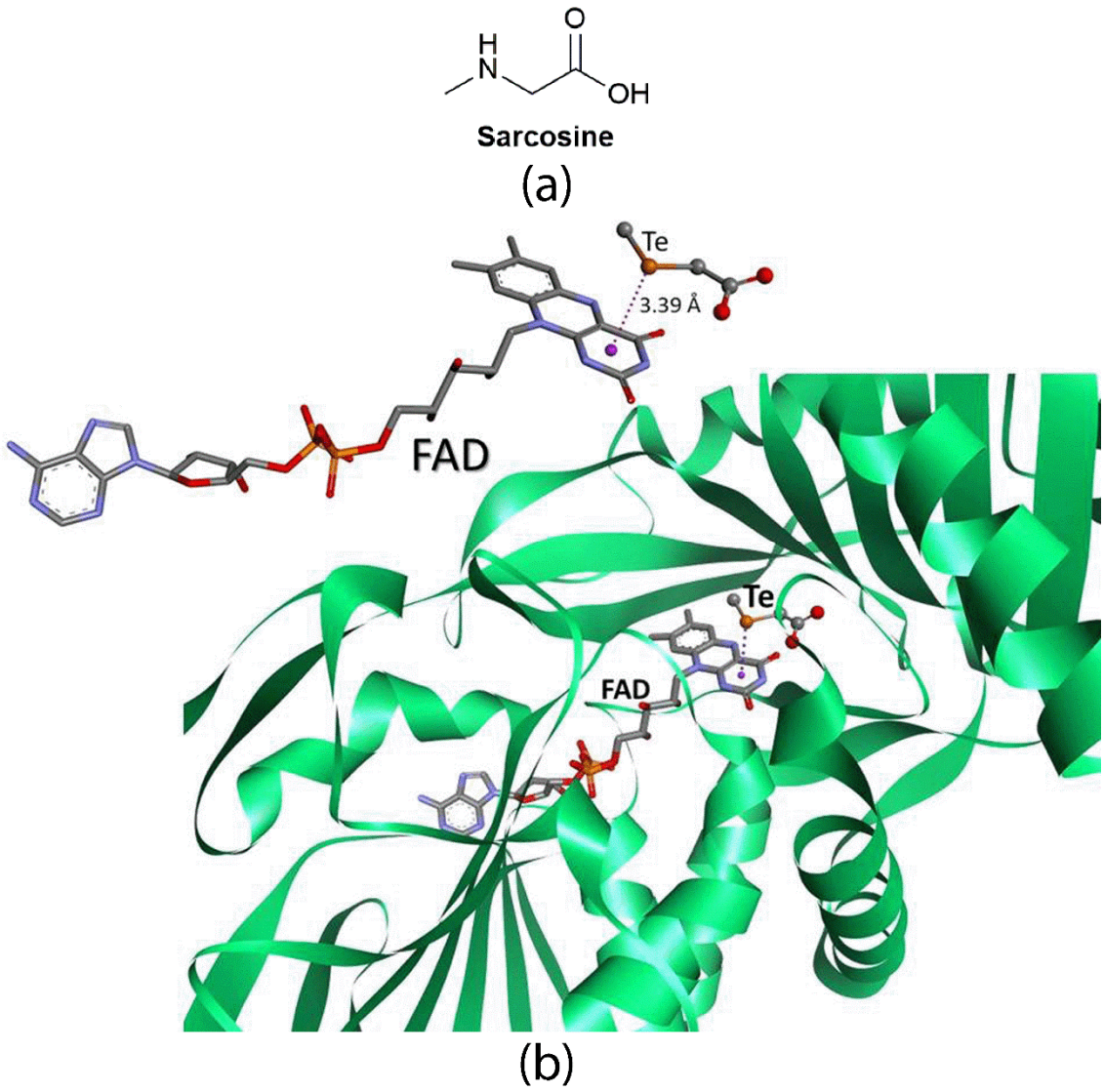

Fig. 27 (a) Chemical diagram of sarcosine, and (b) image representing the interaction of a tellurium(II)-substituted sacrosinate anion with the active site (FAD) of sarcosine oxidase; insert (above): detail of the tellurium(II)…π(pyrimidinyl)interaction.